Geophys. J. Int. (2009) **178,** 106–122 doi: 10.1111/j.1365-246X.2009.04149.x

A palaeomagnetic and $^{40}Ar/^{39}Ar$ study of late precambrian sills in the SW part of the Amazonian craton: Amazonia in the Rodinia reconstruction

S.-Å. Elming,[1] M. S. D'Agrella-Filho,[2] L. M. Page,[3] E. Tohver,[4,5] R. I. F. Trindade,[2] I. I. G. Pacca,[2] M. C. Geraldes[5] and W. Teixeira[6]

[1]*Department of Applied Chemistry and Geosciences, Luleå University of Technology,* S-97187 *Luleå, Sweden. E-mail: sten-ake.elming@ltu.se*
[2]*Departamento de Geofisica., IAG, Universidade de São Paulo, Rua do Matão* 1226, 05508-090, *São Paulo, Brazil*
[3]*Department of Geology, University of Lund,* 22362 *Lund, Sweden*
[4]*School of Earth and Geographical Sciences, University of Western Australia,* 35 *Stirling Hwy, Crawley, WA 6009, Australia*
[5]*Faculdade de Geologia, UERJ, Rio de Janeiro, RJ, Brazil*
[6]*Instituto de Geociências, Universidade de São Paulo, Rua do Lago* 562, *São Paulo,* 05508–080, *SP, Brazil*

Accepted 2009 February 10. Received 2009 February 10, in original form 2007 August 23

SUMMARY

A new key palaeomagnetic pole (Plat. = 64.3°S, Plon. = 271.0°E, N = 14, A_{95} = 9.2°; Q = 5) is calculated from a primary magnetization isolated in early Neoproterozoic Aguapei basic sills and dykes hosted by 1.3–1.0 Ga sedimentary rocks from the southwestern part of the Amazon craton. The characteristic remanence carried by stable, pseudo-single domain titanomagnetite shows two antipodal polarities that pass a reversals test. Magnetic anisotropy for most sites shows fabric orientations that are typical of sills, with horizontal magnetic foliations concordant to the flat-lying bedding of the host sedimentary rocks. $^{40}Ar/^{39}Ar$ analyses for one of the sills reveal a well-defined plateau age at 981 ± 2 Myr. A tectonic reconstruction for Amazonia relative Laurentia based on this new pole 'is consistent with' a position of the present northwestern part of Amazonia attached with eastern Laurentia close to Greenland at *ca.* 981 Ma. On basis of palaeomagnetic and geological data, we propose a scenario where Amazonia moved northeastwards along the present southeast coast of Laurentia from *ca.* 1200 to 980 Ma. By 980 Ma, Amazonia is placed alongside Laurentia and Baltica, in a position similar to other reconstructions of Rodinia but with a significantly different orientation.

Key words: Magnetic fabrics and anisotropy; Palaeomagnetism applied to tectonics; Rock and mineral magnetism.

INTRODUCTION

The assembly of continents into a late Precambrian supercontinent has been suggested in a number of studies (e.g. Piper 1976; McMenamin & McMenamin 1990; Dalziel 1991; Hoffman 1991; Dalziel *et al.* 2000). The Rodinia hypothesis is widely acknowledged in the literature, although the configuration and timing of breakup of this supercontinent are still widely debated. The geometry of Rodinia is mostly modelled on the basis of *ca*. 1350–1000 Ma orogenic belts and tectonic links between mobile belts across cratonic margins. As palaeomagnetism is the only tool for reconstructing latitudinal positions and orientations of the cratons, it plays a key role for the reconstruction of Rodinia. However, reliable palaeomagnetic data are sparse for many of the continents during the time interval of assembly and breakup of the supercontinent, which reduces the possibility of testing proposed configurations (e.g. Buchan *et al.* 2001; Pesonen *et al.* 2003; Meert & Lieberman 2004). The Amazonian craton forms an important part in the Rodinia reconstruction, and distinct tectonic models of relations with Laurentia and Baltica have been suggested (e.g. Priem *et al.* 1989; Dalziel 1991, 1992; Hoffman 1991; Sadowski & Bettencourt 1996; D'Agrella Filho *et al.* 1998; Dalziel *et al.* 2000). However, the number of palaeomagnetic poles from Amazonia is very limited, and the database for palaeomagnetic tests is, thus, restricted to results from *ca*. 1.2 Ga gabbros and basalts of the Nova Floresta Formation (Tohver *et al.* 2002) and sedimentary rocks of the Aguapéi Group, southwestern Amazonia (D'Agrella-Filho *et al.* 2008), which suggests a juxtaposition with Laurentia along its present Grenville margin.

In our study of basic sills and dykes from SW Amazonia, we present new, reliable palaeomagnetic data from the early Neoproterozoic Grenville interval. We use these new data to test the models of a long-lasting tectonic relation between Amazonia, Laurentia and Baltica. Our findings indicate that the southwestern part of Amazonia may have been attached to eastern Laurentia (Greenland) at *ca*. 980 Ma.

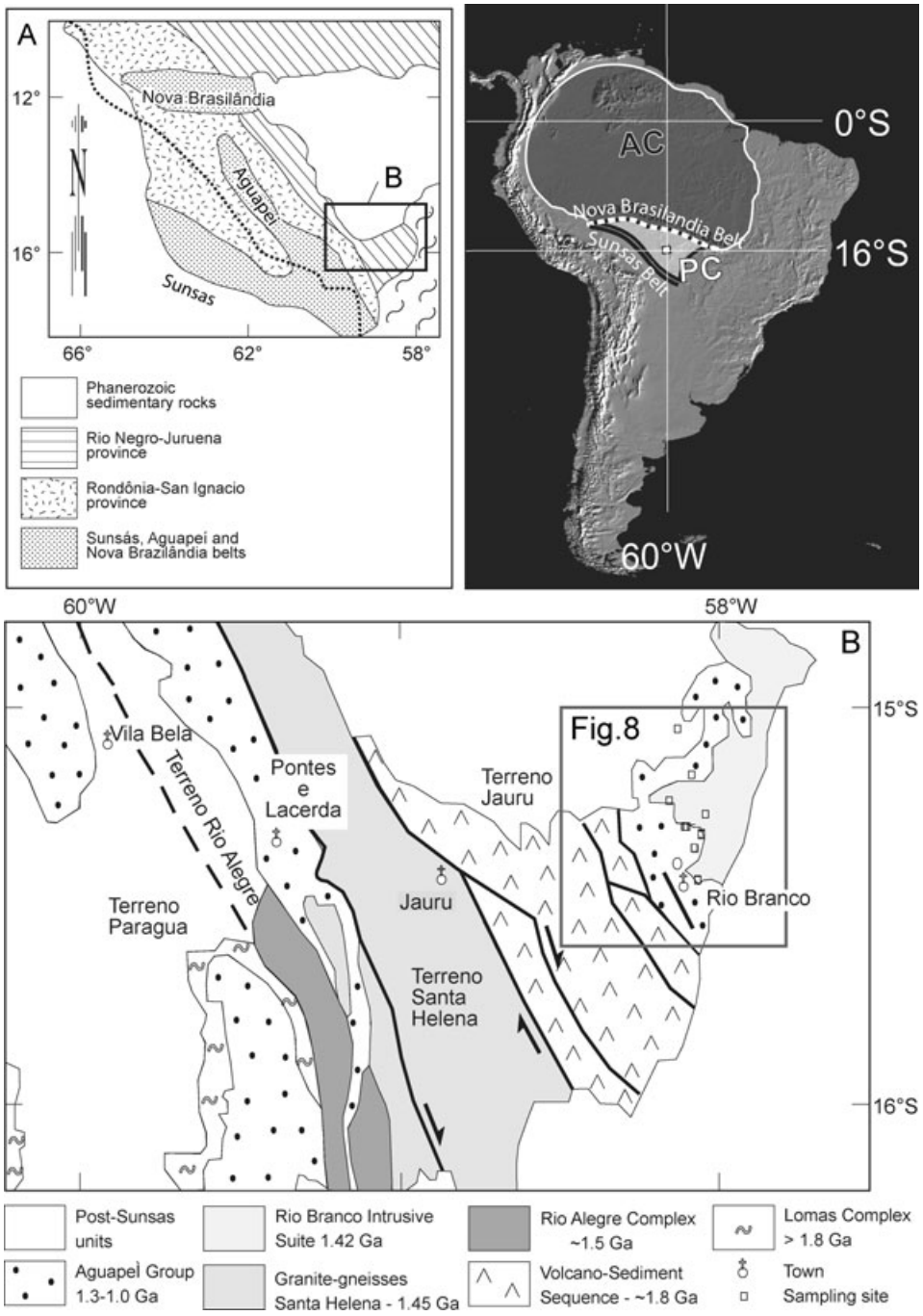

Figure 1. (a) and (b) Map of the geology of southwestern Amazonia. Panel (b) shows the location of sites for the palaeomagnetic sampling and the framed area is used in Fig. 8 (adapted from Saes 1999).

GEOLOGY AND SAMPLING

The Amazonian Craton is composed of an Archaean nucleous and Paleoproterozoic accretionary belts that young successively to the SW (e.g. Cordani & Teixeira 2007): the 1.8–1.6 Gyr old Rio Negro-Juruena province (Fig. 1a) is bordered towards the SW by the 1.5–1.3 Gyr old Rondonian-San Ignacio province and the *ca*. 1.3–0.9 Gyr old Sunsás province that forms the SW margin of the craton. The Sunsas belt *sensu strictu* has long been considered a counterpart of the Grenville belt in the tectonic reconstructions between Amazonia and Laurentia (e.g. Hoffman 1991). The Sunsas province, according to some models, comprises three separate belts: the 1.05–1.1 Gyr old Sunsas belt proper of west-central Bolivia that forms the southern border of the Paragua craton (Litherland *et al.* 1989; Boger *et al.* 2005); the intracratonic Aguapeí belt where *ca*. 1.15 Gyr old sediments were deformed at *ca*. 950 Ma (Saes 1999; Saes & Leite 1993; Ruiz 2005) and the 1.1 Gyr old Nova Brasilândia metasedimentary belt that forms the northern margin of the Paragua craton and is interpreted as a suture zone with the Amazon metaigneous basement to the north (Tohver *et al.* 2004a; Tohver *et al.* 2005a). An alternative approach (Cordani & Teixeira 2007) considers the Sunsas orogenic belt as restricted to the southern bounds of the Paraguá craton, structurally marked by shear and mylonitic zones, granitoid

rocks and supracrustal sequences and reactivated basement rocks. The Sunsas belt originated in an extensional environment, consisting of a passive margin sedimentary sequence (the Vibosi and Sunsas belts) that was subsequently deformed during a continental collision and intruded by granitic suites accompanying extensive deformation along the tectonic zones, followed by the emplacement of post-tectonic plutons. According to Cordani & Teixeira (2007), the cratonic area in Brazil the Nova Brazilandia and the Aguapeí belts, dated at *ca*. 1160 Ma (Rizzotto *et al.* 2001; Santos 2003), were deformed in rift-type structures that later were affected by transpression and crustal shortening and granite intrusions due to the Sunsas collision. The related tectonic reactivation led to anorogenic magmatism (e.g. granites, sills and dykes) in the tectonically stable crust, such as the widespread anorogenic granitic magmatism of the Younger Granites of Rondonia, also referred as the Rondonia Tin Province (ages between 970 and 1100 Ma; Priem *et al.* 1989; Bettencourt *et al.* 1999), the coeval plutons in Mato Grosso as well as emplacement of the 990 Ma Rincon del Tigre mafic-ultramafic complex in Bolivia (Annels *et al*. 1986). Cordani & Teixeira (2007) therefore considered these intraplate tectonomagmatic events as tectonic reflections of the Sunsas orogeny over the stable foreland.

The Amazon basement itself was deformed earlier, 1.15–1.2 Ga, on basis of $^{40}Ar/^{39}Ar$ and feldspar thermometry data from a wide area of strike-slip shear active at temperatures of 450–550°C (Tohver *et al.* 2005b).

The present work is focused in the Brazilian state of Mato Grosso, southeast of the 1.1 Gyr old suture zone, where Proterozoic basement rocks that crop out in the Jauru terrane are interpreted by Geraldes *et al.* (2001) to be a SE extension of the Rio Negro-Juruena province. The geology of the Mato Grosso region includes various rock types, with ages ranging from 1.80–1.75 Gyr for the Jauru basement to the 1.52–1.47 Gyr rocks of the Rio Alegre Complex (Fig. 1b). Intrusion of the Santa Helena batholith has been dated at 1.45 – 1.42 Gyr, using U–Pb analysis of zircon by Geraldes *et al.* (2004), who considered the Rio Branco intrusions to be coeval, mafic representatives of a bimodal suite. The Aguapei Group sediments comprise quartzose sandstone and conglomerates of the basal Fortuna Formation, overlain by pelitic rocks and fine lithic, sub-arkosic rocks of the Vale da Promissão Formation, topped by quartz sandstones of the Morro Cristalina Formation (Souza & Hildered 1980; Saes 1999). A deformational event folded and faulted these sedimentary rocks under lower greenschist conditions within the central portion of the *ca*. 50-km-wide Aguapei belt. The external margins of this deformed zone are found to the west along the Brazil–Bolivia frontier and to the east, close to the Brazilian town of Rio Branco, where nearly undeformed, subhorizontal layers with minimal metamorphism are observed (Fig. 1).

Basaltic dykes and sills are found intruding into the flat-lying Aguapei Group sediments, including the Fortuna Formation and Vale da Promissao Formation near the town of Rio Branco. The sills form 1 to 5 m thick beds that intrude parallel to the sedimentary bedding, with a mesocratic aspect ranging from dark grey to black. The grainsize ranges from fine to medium, and the composition varies from gabbro to quartz-monzodiorite (Ruiz 2005). Plagioclase (labradorite-andesine) occurs commonly in the matrix as tabular euhedral to subeuhedral crystals and less commonly as phenocrysts up to 5 cm. The primary mineralogy consists of plagioclase, hornblende, biotite, orthoclase, quartz and, rarely, olivine. Cumulative and ophitic textures are common, and the accessory minerals are represented by zircon, titanite, magnetite, ilmenite and pyrite. Geochemical data suggest that the sills are typical of intracratonic origin (Ruiz 2005). K–Ar dating on plagioclase and whole rock of the sills suggests ages between 1015 ± 17 and 875 ± 21 Myr (Barros *et al.* 1982; Ruiz 1992, 2005). Hornblende and biotite $^{40}Ar/^{39}Ar$ data from basement rocks preserve igneous crystalline ages, indicating a very low degree of exhumation (<5 km) for this region and the absence of high grade metamorphism during the Grenvillian interval (Tohver *et al.* 2006a). From the standpoint of paleomagnetism, this information signifies that this long-stable region has the potential to preserve ancient directions from the Grenvillian and pre-Grenvillian interval and has been part of the Amazon craton since at least *ca*. 1.15 Ga.

METHODS

Palaeomagnetism

Basic sills have been sampled in 14 sites (Fig. 1b), using a portable rock drill. A total of 108 samples were collected and oriented with both sun and magnetic compasses. Standard alternating field (AF) and thermal demagnetization techniques were applied and the laboratory work was done in the Palaeomagnetic laboratories at the Universidade de São Paulo, Brazil, and Luleå University of Technology, Sweden. A Schonstedt TSD-1 and a magnetic measurements MMTD60 furnace (peak temperature within ±2 °C, heating time of 1 hr) were used for the stepwise thermal demagnetizations with AF demagnetization carried out in conjunction with use of the SQUID (2G-DC) magnetometer, which was also used to measure magnetic remanence. For samples with high NRM intensities, a Molspin Spinner magnetometer was used to measure remanent magnetization, and demagnetization was conducted using a Molspin AF-demagnetizer. At São Paulo, the instruments are housed in a magnetically shielded room with an ambient field <1000 nT. The anisotropy of magnetic susceptibility (AMS) was measured to define the magnetic fabric of the rocks using a Molspin Minissep instrument. The technique of Jelínek (1978) was used for the statistical analyses of the AMS data. Low field magnetic susceptibility variation with temperature was obtained using a Bartington (MS2W) instrument. The magnetic susceptibility was measured during continuous heating and cooling of specimens up to 700 °C. The Curie temperature determined from these experiments was compared with the unblocking temperatures determined from the thermal demagnetizations to identify the carriers of remanent magnetization. The hysteresis properties were measured using a Molspin Vibrating Sample Magnetometer (VSM) to determine the domain state of the remanence carriers.

Demagnetization results were analysed using orthogonal plots (Zijderveld 1967) and stereographic projections and the components of remanence were defined using principal component analysis (Kirschvink 1980). At least four demagnetization steps were

Table 1. $^{40}Ar/^{39}Ar$ data for the Aguapei sills and dykes, integrated and whole rock (WR) plateau force-fit ages.

Site/sample	Rock	Integrated age (Ma)	WR plateau (P) force-fit age (F) (Ma)
3/3c3	Basic dyke	988 ± 2	1035 ± 3 (F)
3/3c4	Basic dyke	970.3 ± 1.7	1025 ± 8 (F)
8/8e3	Basic sill	877 ± 1.8	922 ± 2 (F)
8/8e4	Basic sill	878.3 ± 1.8	908 ± 11 (F)
8/8f2	Basic sill	976 ± 2	981 ± 2 (P)

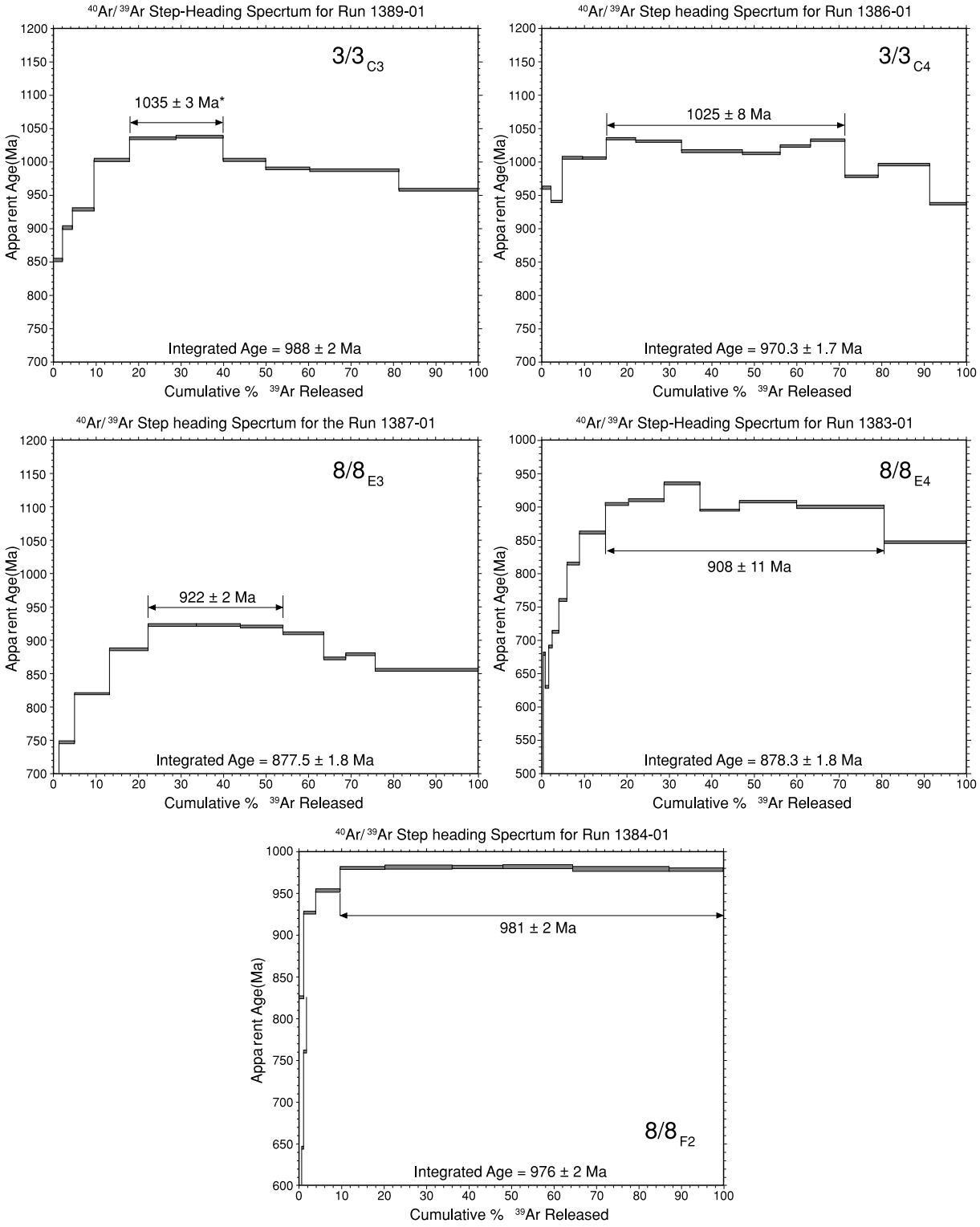

Figure 2. $^{40}Ar/^{39}Ar$ age spectra from whole-rock basic dyke ($3/3_{c3}$ and $3/3_{c4}$) and sill ($8/8_{E3}$, $8/8_{E4}$ and $8/8_{F2}$). The samples are obtained from palaeomagnetic drill cores. See text for details.

used to calculate vectors in the orthogonal diagrams, and an upper limit for mean angular deviation (MAD) of 8° was used, although most vectors were very well defined with MAD generally <3°. The site and formation mean directions were calculated from AF data using Fisher statistics (Fisher 1953).

$^{40}Ar/^{39}Ar$ dating

Palaeomagnetic core samples of basalt dykes and sills were used for $^{40}Ar/^{39}Ar$ analysis at the Geochronology laboratory at University of Lund, Sweden. The cores were crushed, cleaned and sieved to a

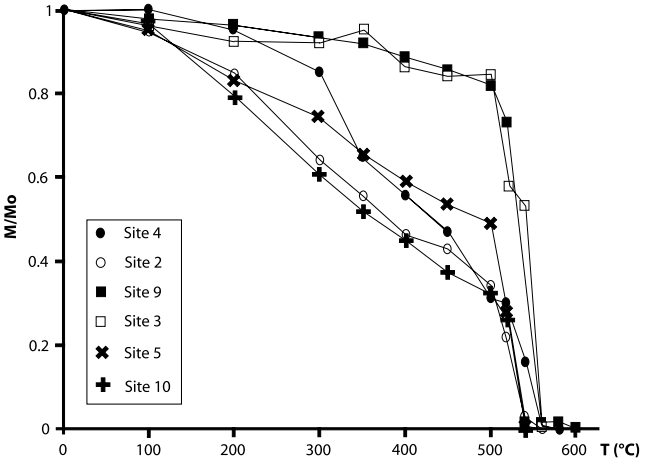

Figure 3. Examples of thermal demagnetization of sills and a basic dyke (site 3). The ratio M/M_0 denotes the normalized intensity of remanent magnetization.

0.25–0.5 mm size fraction, and several milligrams of the whole rock material were irradiated together with the DRA-2 sanidine standard (25.26 Ma; Wijbrans *et al.* 1995, recalculated following Renne *et al.* 1998) for 35 hr at the NRG-Petten HFR RODEO facility in the Netherlands. *J*-values (the irradiation parameter) were calculated with a precision of 0.25 per cent. Since there is a high flux at the cadmium shielded facility at NRG-Patten, the irradiation time can be held relatively short. Frequently, an inhouse 980 Ma muscovite standard has been used to check the results from dating of rocks older than the sanidine standard. There is no indication of influence on the determined ages using the young standard.

The $^{40}Ar/^{39}Ar$ laboratory at the University of Lund employs a Micromass-5400 mass spectrometer with a Faraday cup and an electron multiplier. A metal extraction line, which contains two SAES C50-ST101 Zr-Al getters and a cold finger cooled to –155 °C by a Polycold P100 cryogenic refrigeration unit is also present. A few mg of the whole rock samples were loaded into a copper planchette that consists of several 3 mm holes. The samples were step-heated using a defocused 50W CO_2 laser. Sample clean-up time was 5 minutes, using the two hot Zr-Al SAES getters and the cold finger. The laser was rastered over the samples to provide even heating of all grains. Time zero regressions were fitted to data collected from 10 scans over the mass range of 40–36. Peak heights and backgrounds were corrected for mass discrimination, isotopic decay and interfering nucleogenic Ca-, K- and Cl-derived isotopes. Isotopic production values for the cadmium lined position in the Petten reactor are $^{36}Ar/^{37}Ar_{(Ca)} = 0.000270$, $^{39}Ar/^{37}Ar_{(Ca)} = 0.000699$ and $^{40}Ar/^{39}Ar_{(K)} = 0.00183$. ^{40}Ar blanks were calculated before every new sample and after every three sample steps. ^{40}Ar blanks were between 5.0×10^{-16} and 3×10^{-16}. Blank values for masses 36–39 were all less than 7×10^{-18}. Blank values were subtracted for all incremental steps from the sample signal. Age plateaus were determined using the criteria of Dalrymple & Lanphere (1971),

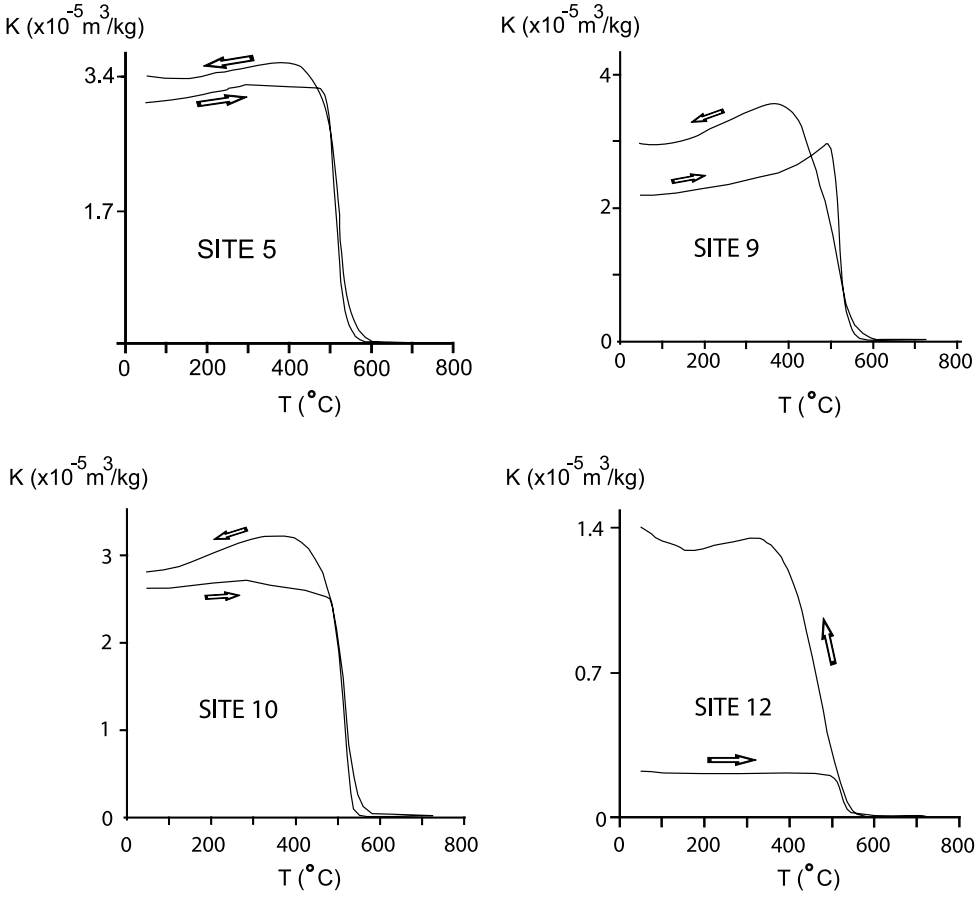

Figure 4. Thermomagnetic curves (susceptibility versus temperature) for sill samples from four sites. Note the increase in susceptibility during cooling of the sample from site 12, possibly indicating titanomaghemite to be one of the magnetic minerals.

which specify the presence of at least three contiguous incremental heating steps with statistically indistinguishable ages and constituting greater than 50 per cent of the total ^{39}Ar released during the experiment.

RESULTS

Geochronology

$^{40}Ar/^{39}Ar$ whole rock age analyses were performed on five samples (Table 1), three from site 8 and two from site 3. One of the samples from site 8 yield a plateau age of 981 ± 2 Myr (sample 8_{F2}; Fig. 2), according to the criteria of Dalrymple & Lanphere (1971). We interpret the 981 Ma plateau age to represent the cooling age of the sill, as suggested by its primary mineralogy. Two other samples of the same site yield disturbed age spectra with a staircase pattern of increasing age from the initial fractions over the first 20 per cent of degassed ^{39}Ar, suggestive of significant argon loss through diffusion (samples 8_{E3} and 8_{E4}, Fig. 2). Pseudo-plateau ages obtained for these samples suggest a minimum age of 922 ± 2 and 908 ± 11 Myr, respectively. The two samples from site 3 (3_{C3} and 3_{C4}) yield disturbed spectra with pseudo-plateau ages for these samples of 1035 ± 3 and 1025 ± 8 Myr (Fig. 2), respectively, thereby interpreted as minimum ages. The difference in minimum ages obtained for the sites suggests that the rock at site 3 is older than the rock at site 8.

Magnetic carriers

Thermal demagnetization reveals a range of unblocking temperatures (T_{ub}) of *ca*. 530–550 °C (Fig. 3). However, a widely distributed T_{ub} spectrum is observed for samples from nine of the sites, for which up to ∼70 per cent of the remanence is erased at temperatures below 525 °C. Susceptibility versus temperature measurements have been conducted on samples from all sites and the curves (Fig. 4) indicate Curie temperatures in the range 530–550 °C, suggesting titanomagnetite to be the magnetic carrier. The increase in susceptibility during cooling of samples from the site 12 could indicate titanomaghemite to be one of the magnetic minerals, as the heating-cooling curve for titanomagnetite (site 5) is expected to be reversible (Dunlop & Özdemir 1997).

The properties determined from the hysteresis measurements show a clear trend in the ratio of saturation remanent magnetization (M_{rs}) and saturation magnetization (M_s), M_{rs}/M_s, versus the ratio of coercivity of remanence (H_{cr}) and coercive force (H_c), H_{cr}/H_c. The diagram (Fig. 5) indicates grainsizes of the remanence carrying minerals trending from the transistion of single domain—pseudo-single domain (SD–PSD) to multidomain (MD) grains. However, the overall majority of samples plot well within the PSD part of the diagram (Day *et al.* 1977).

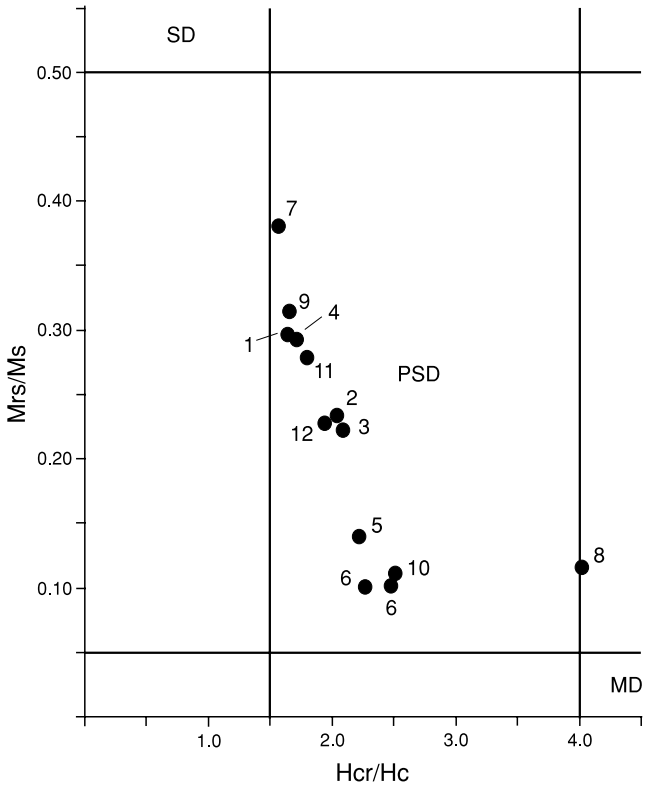

Figure 5. Hysteresis ratios measured for the sills and dykes and plotted in a Day-diagram (Day *et al.* 1977). M_{rs}, saturation remanent magnetization; M_s, saturation magnetization; H_c, coercive force; H_{cr}, coercivity of remanence; SD, single domain; PSD, pseudo single domain; MD, multidomain. The numbers refer to the site of the sample.

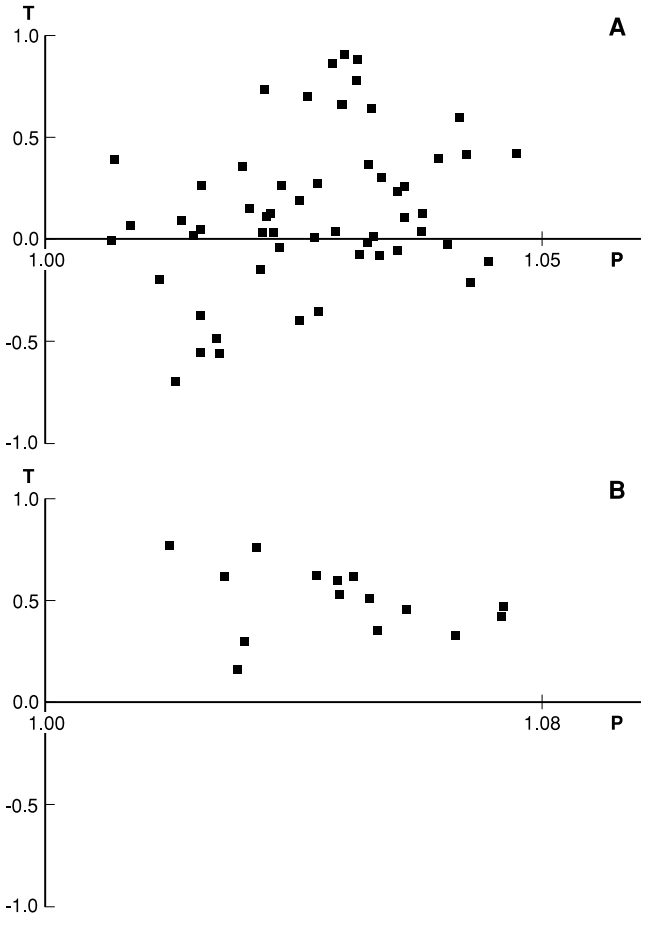

Figure 6. Data from anisotropy of magnetic susceptibility (AMS) plotted in a *P*–*T* diagram (Jelinek 1981) expressing the shape of the susceptibility ellipsoid. *P* denotes the degree of anisotropy. An oblate ellipsoid is expressed by $0 < T < 1$, and a prolate ellipsoid is expressed by $-1 < T < 0$. A, Sills; B, Dykes. Note that for most samples, the magnetic fabric is oblate.

Anisotropy of magnetic susceptibility

The bulk mean magnetic susceptibility of the basic rocks varies from approximately 0.16×10^{-3} SI to 2.5×10^{-3}, with the majority of site means higher than 1.0×10^{-3}, suggesting a predominantly ferromagnetic origin of the susceptibility. The degree of anisotropy is less than 10 per cent for the rocks of our study ($P < 1.08$; Fig. 6), typical of igneous rocks with primary magnetic fabric (Hrouda 1982). The shape of the anisotropy ellipsoid is expressed by the shape parameter T (Jelinek 1981), for which a prolate ellipsoid is expressed by $-1 < T < 0$ and an oblate ellipsoid is expressed by $0 < T < 1$. In most of the sites the T values are positive, indicating that the magnetic fabric of the studied rocks is predominantly oblate (Fig. 6).

The majority of sites are characterized by k_{min} axes that cluster in subvertical directions (Fig. 7a). We interpret the AMS data as a primary flow indicator (Knight & Walker 1988; Tauxe *et al.* 1998), with the directions of k_{max} indicating the principal magmatic flow direction. The shallow, subhorizontal dip of the magnetic foliation planes suggests sill geometry for these rocks, with flow directions principally in the NE–SW and NW–SE directions. The AMS data from sites 1 and 2 reveal neither a typical sill nor a dyke pattern of the susceptibility with intermediate dips of the k_{min} axes.

In sites 3, 4 and 6, k_{min} axes are very shallow dipping ((Table 2), and two of them (3 and 4) are characterized by oblate magnetic fabrics (Figs 6b and 7b), indicating that these are dykes rather than sills. Contrary to the shallow magma flow directions that vary from between NE to NW, in the sills the magma flow direction (i.e., K1) in the dykes is subvertical. The foliation planes that express the dyke planes at sites 3 and 4 strike ENE (~73°E; Fig. 8). The direction of the k_{min} axes (pole of the dyke plane) at site 6 suggests a dyke trend of 130°E. For sites 1 and 12, the directions of the k_{int} and k_{min} form a girdle and the directions of the k_{max} axes are at dec. = 43°E, inc. = 26° and dec. = 320°E, inc. = 2°, respectively. The AMS patterns from the rock in sites 13 and 14 are more isotropic, and no preferred orientations of the axes can be defined. Aside from the light that these data shed on magmatic flow patterns, the AMS data suggest a tectonically undisturbed magmatic body, where the k_{min} directions for dykes, sills and flows approximate the pole of the flow plane (e.g. Knight & Walker 1988; Elming & Mattsson 2001). More importantly, the AMS data demonstrate that no tilt corrections are necessary for the paleomagnetic directions.

Palaeomagnetism

The remanent magnetization, apparently hosted by titanomagnetite and titanomaghemite, is commonly of high coercivity with median destructive fields (MDF) of the order of 15–30 mT (Fig. 9), supportive of a PSD behaviour of the remanent magnetization, which is inferred to be stable over geological time scales. The unblocking temperature (T_{ub}) spectrum varies from wide to rather narrow (Figs 3 and 9). However, characteristic magnetizations are, in most cases, isolated in T_{ub} of 500–580 °C.

In these basic sills, there are generally two components of magnetization. Thermal treatment does not completely eliminate the secondary magnetization even at temperatures close to the Curie temperature of magnetite–titanomagnetite, probably due to overlapping T_{ub} spectra of the two components, which resolves only an

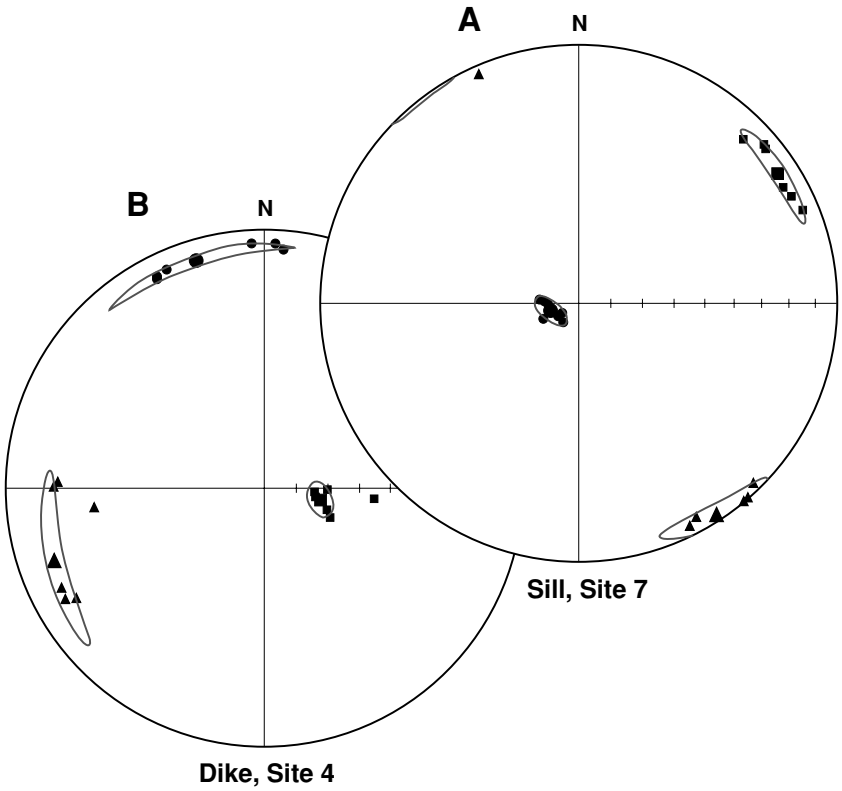

Figure 7. Examples of lower hemisphere equal area projection plots of directions of the maximum (■) intermediate (▲) and minimum (●) susceptibility axes. The ovals are 95 per cent confidence limits about each axis of the site mean susceptibility ellipsoid. A typical plot for a sill is shown in panel (a), whereas a plot for a dyke is shown in panel (b).

Table 2. Palaeomagnetic and AMS data for basic sills and dykes in the Rio Branco area, southwestern Amazonia.

Site, rock		Glat/Glon (S°/E°)	*N*, *n*	Decl.	Incl.	α_{95}	*k*	N, R	Plat (N°)	Plon (E°)	A95	L/F	k_{max} decl.	k_{max} incl.	k_{min} decl.	k_{min} incl.	*P*	Comments to AMS data
1, ?		15.299/301.890	1, 5	32.7	−45.8	18.6	18	M	−57.4	238.8	18.9	F	43.0	26.0	299.0	28.0	1.015	girdle min int
2, ?	a-c	15.299/301.885	1, 6	3.0	−54.7	19.5	13	M	−69.9	294.7	23.2	F	36.0	53.0	285.0	15.0	1.047	
	d-f		1, 3									F	115.0	7.0	217.0	61.0	1.030	
3, dyke,	LHc	15.299/301.847	1, 6	46.0	−34.0	12.3	30	N	−46.0	223.1	10.6	F	70.0	61.0	164.0	2.0	1.063	Trend of F-plane 254E
	HHc		1, 6	140.0	−13.6	5.7	138	?	44.6	238.3	4.2							
4, dyke,	LHc	15.299/301.884	1, 9	189.6	63.7	15.5	12	M	−58.9	288.8	21.9	F	101.0	72.0	343.0	9.0	1.019	Trend of F-plane 73E, A-F
	HHc		1, 6	351.1	9.2	7.9	73	N?	68.2	277.3	5.7	F	66.0	84.0	280.0	5.0	1.038	Trend of F-plane10E, G-I
5, sill		15.433/301.925	1**, 6	184.8	45.9	5.6	144	R	−77.3	282.1	5.8	F	11.0	13.0	210.0	76.0	1.029	
6, dyke		15.434/301.925	1**, 6	205.7	68.9	12.0	30	R	−47.8	278.7	18.7	L	82.0	87.0	220.0	2.0	1.022	Trend of F-plane 310E
7, sill		15.320/301.937	1*, 6	21.8	−53.6	3.1	482	N	−62.8	259.7	3.6	L/F	56.0	9.0	258.0	81.0	1.041	
8, ?	LHc	15.317/301.936	1, 6	2.4	−26.2	9.8	48	N	−87.2	179.5	7.8	F	312.0	11.0	58.0	54.0	1.009	Poorly defined
	HHc		1*, 6	17.1	−51.4	3.9	291	N	−67.1	262.1	4.4							
9, sill		15.268/301.949	1*, 8	22.0	−50.5	4.5	153	N	−64.3	254.3	5.0	L/F	75.0	10.0	268.0	80.0	1.037	
10, sill		15.234/301.836	1**, 8	143.3	49.2	12.6	20	R	−53.2	1.6	13.6	F	297.0	1.0	33.0	79.0	1.037	
11, sill	HHc	15.354/301.916	1*, 4	2.8	−62.8	8.6	115	N	−61.0	297.8	12.0	F	34.0	9.0	245.0	79.0	1.018	
12, ?		15.316/301.936	1*, 7	11.6	−55.0	3.3	333	N	−67.3	276.9	3.9	L	320.0	2.0	54.0	67.0	1.012	girdle min int
13, ?		15.054/301.862	1**, 9	213.8	65.2	2.1	131	R	−47.4	268.0	6.6							
14, ?		15.169/301.906	1**, 23	202.5	61.8	2.1	205	R	−56.2	271.7	2.9							
Mean N			5*, 31	15.8	−54.8	6.2	152	N	−65.5	269.5	7.4							
Mean R			5**, 52	185.8	60.9	17.3	21	R	−62.9	292.4	23.1							
Mean N+R			10, 83	11.3	−57.9	8.1	37	N, R	−64.7	280.9	10.2							

Note: The site means are calculated from high *Hc* components isolated in AF demagnetizations. Site, rock denotes sill or dyke; Glat/Glon, geographic latitude and longitude of the site; *N*, *n*, number of sites, samples; * (**), sites used for calculating mean of normal (revesed) site means. Decl. (Incl.), mean declination (inclination) of the remanent magnetization; α_{95}, radius of the 95 per cent cone of confidence; *k*, the Fisher precision parameter; *N* (*R*) and *M*, Normal (reversed) and mixed polarity of remanence direction; Plat (Plon), latitude (longitude) of the virtual geomagnetic pole position; A_{95}, half-angle of the 95 per cent circle of confidence of the pole position; L/F, Lineated /foliated magnetic fabric; Kmax decl (incl), declination (inclination) of the maximum susceptibility axis; Kmin decl (incl), declination (inclination) of the minimum susceptibility axis; *P*, degree of anisotropy.

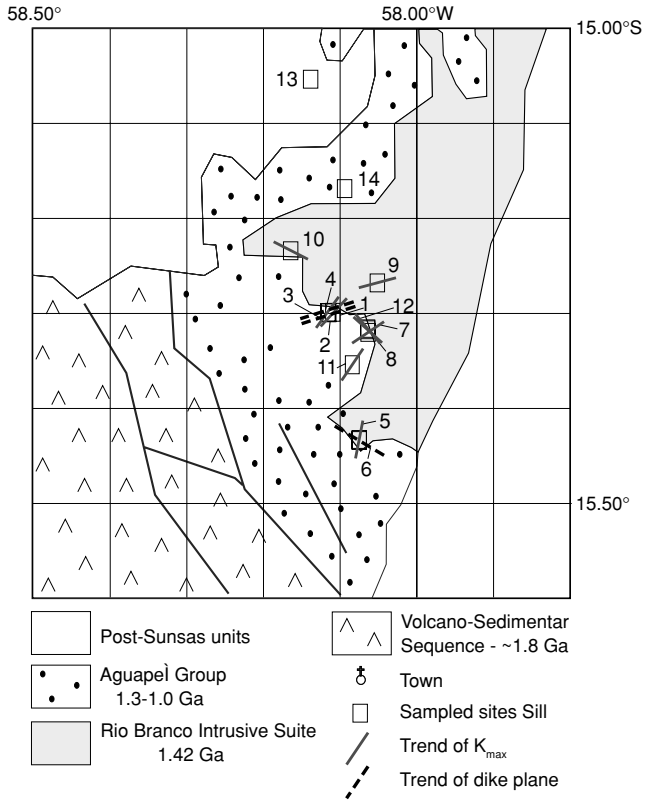

Figure 8. Site mean strike directions of the maximum susceptibility axes indicating flow directions in the sills and strike directions of the dyke planes defined from their magnetic foliation planes.

intermediate direction. The characteristic magnetization is therefore best isolated by AF demagnetization.

The site mean directions are generally well defined with a precision parameter (k; Fisher 1953) generally higher than 40 (12 of 18 sites) and in the 100–500 range for 10 sites (Table 2).

Note that we exclude sites 1 and 2 from the calculation of formation mean because these sites give doubtful AMS-constrained orientations. The poor precision of the mean directions of characteristic magnetizations for these sites ($\alpha_{95} > 18^\circ$ and $k < 20$) may reflect tectonic disturbances within the sites, in keeping with the anomalous AMS orientations.

For sites 3 and 4, two different components of magnetization are identified (Fig. 9), one of which isolated in low H_c and T_{ub} ranges. This low H_c/T_{ub} direction (Table 2) is not significantly different from normal and reversed directions of the sills but different from the expected dipolar field (dec. $= 0^\circ$, incl. $= -28.1^\circ$) and the International Geomagnetic Reference Field (IGRF: dec. $= 345.8^\circ$, incl. $= -12.4^\circ$). However, since this direction is carried by magnetizations with H_c and T_{ub} of $\leq$10 mT and 500 °C, respectively, they may well be of a more recent origin, and these site means are not included in the calculation of the formation mean. The high H_c/T_{ub} components are significantly different from the characteristic magnetizations of the sills (site 3, dec. $= 140^\circ$, inc. $= -13.6^\circ$; site 4, dec. $= 351.1^\circ$, inc. $= 9.2^\circ$). AMS data indicate that these rocks are subvertical dykes, and the $^{40}Ar/^{39}Ar$ pseudo-plateau ages ($\geq$1035 Myr) indicate the dyke at site 3 to be older than the sills, although no good plateau age could be defined. These directions have no resemblance with the moderate to steep remanence directions obtained for the 1150 Ma (D'Agrella-Filho *et al.* 2008) and the 1200 Ma (Tohver *et al.* 2002) rocks in the region, and the only published remanence directions from Amazonia similar to those of sites 3 and 4 are from the *ca.* 1640 Myr old Rio Aro, Roraima and La Escalera basic dykes from the Venezuelan part of Amazonia (Hargraves 1968; Onstott *et al.* 1984), which were suggested to carry primary magnetizations. The disturbed age spectra of site 3 suggests that the dykes may have been reheated by the nearby sill, which resulted in an almost complete resetting of the argon system, although the temperature was not high enough to produce a magnetic overprint of the original magnetization.

The AMS data suggest that the rock at site 6 is a dyke with a direction of k_{max} indicating a subvertical magma flow. This dyke hosts a characteristic magnetization (high H_c and T_{ub}) that falls into the group of reversed sill directions. We suggest that this dyke was emplaced (and magnetized) contemporaneously with the sills, that is, a feeder dyke for the sills. This may be supported by the almost perpendicular flow directions indicated for the sill at site 5, relative to the trend of the neighbouring dyke at site 6 (Fig. 8).

The samples from site 14 were collected from three different levels of a thick (10–15 m) section of the sill. The site mean directions from the three levels are well defined and not significantly different, suggesting a rapid cooling of the sill. The samples are therefore treated as collected from one single site.

The formation mean is, thus, calculated from the site means of sites 5–14. Dual polarities of the characteristic remanence are observed; a normal polarity direction with a well-defined mean of sites at dec. $= 15.8^\circ$, inc. $= -54.8^\circ$ ($\alpha_{95} = 6.2^\circ$) and a reversed polarity direction with a less precise mean at dec. $= 185.8^\circ$, inc. $= 60.9^\circ$ ($\alpha_{95} = 17.3^\circ$) (Fig. 10; Table 2).

Inverting the reversed polarity direction demonstrates that the mean directions of the two magnetic polarities are not significantly different, as seen from the overlapping cones of confidence (Fig. 10; McFadden & Lowes 1981). This fact justifies the calculation of a mean of site means, including both polarities (dec. $= 11.3^\circ$, inc. $= -57.9^\circ$, $\alpha_{95} = 8.1^\circ$). The positive reversal test for this result also signifies that the remanences were acquired over a substantial interval of geological time ($>10^3$ yr), enough to have averaged out the effects of secular variation. In addition, the preservation of a dual polarity result from unmetamorphosed igneous rocks suggests that the magnetic remanence was acquired when the rock formed. We argue that the characteristic magnetization of the sills is primary, and there seems to be no high temperature event in the region resetting the high T_{ub} magnetizations of the sills and dykes. A palaeomagnetic pole position is calculated from the mean of the normal and reversed site mean directions at 280.9°E and 64.7°S ($N = 10$, $A_{95} = 10.2^\circ$; Table 2). This palaeomagnetic pole position thus represents a primary magnetization with an Ar^{40}/Ar^{39} age of *ca*. 981 Myr as determined from the sill at site 8. The pole has a quality factor (Q) of 5 (Van der Voo 1990), that is, (1) the rock is well dated; (2) the number of samples is sufficient and the statistical demands are fulfilled; (3) the samples have been adequately demagnetized; (4) there is a structural control and a tectonic coherence with the craton and (5) reversals have occured.

DISCUSSION

There are very few Precambrian poles for the Amazonian shield. Tohver *et al.* (2002) presented a reliable 1200 Ma pole for Amazonia from a study of basaltic sills, the Nova Floresta Formation, in the western part of the Amazon craton. A new pole for 1150 Ma has recently been reported for the Amazon craton, based on a study of the Aguapeí Group (D'Agrella-Filho *et al.* 2008).

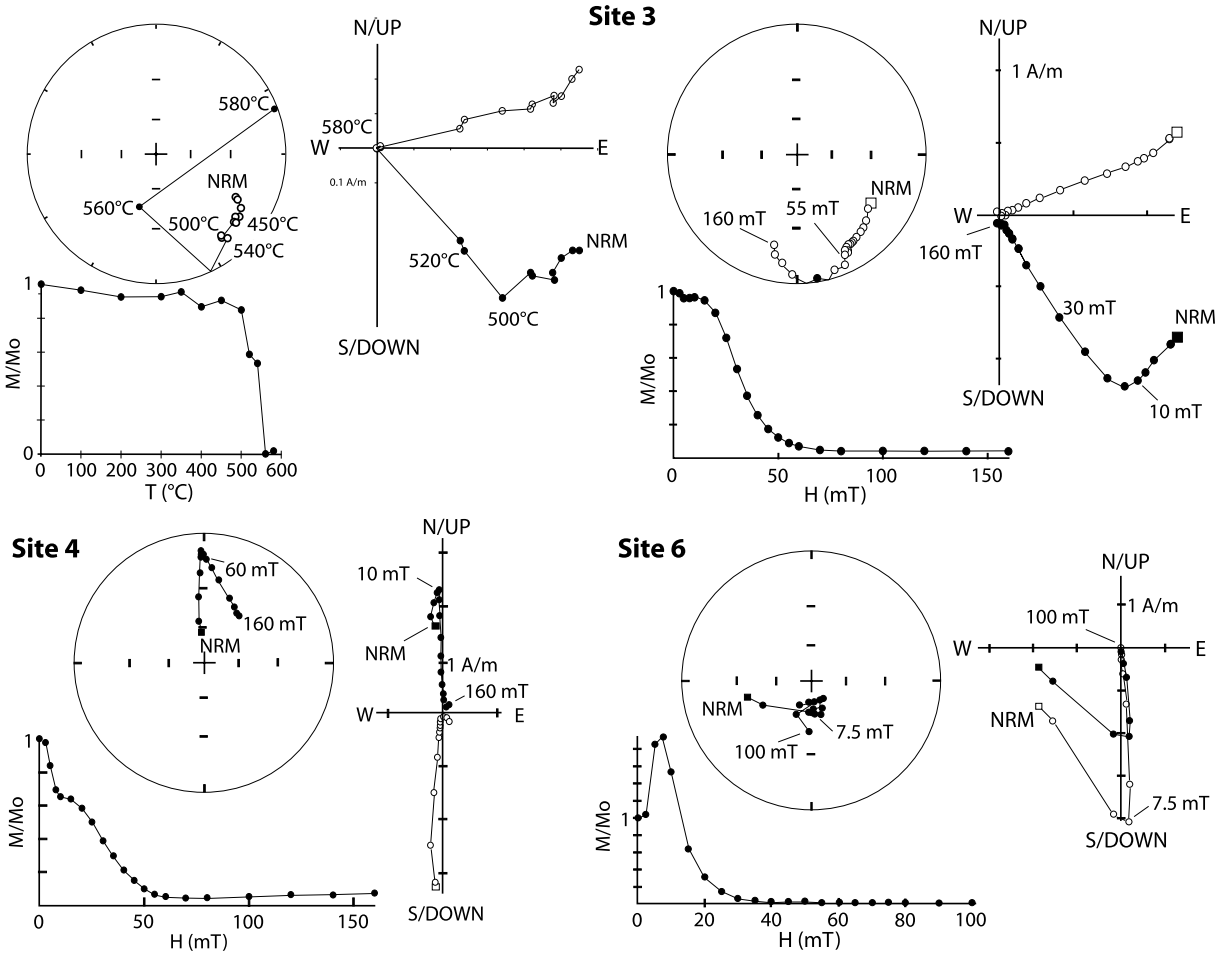

Figure 9. Examples of remanence behaviour during progressive alternating field and thermal demagnetization for sites 3, 4, 5, 6 and 12. Open (closed) symbols in the vector plots denote vertical (horizontal) projections. Open (closed) symbols in the stereographic projections denote negative (positive) inclinations of the remanence vector.

These poles are the only poles for Amazonia in the interval 1200–800 Ma (see Tohver *et al.* 2006b). Therefore, our new pole is an important contribution to tectonic reconstructions of the Rodinia supercontinent, given the prominence of Amazonia in these reconstructions. To test models of Rodinia with respect to Amazonia, poles of similar age are needed from the three key cratons that are considered to be linked by Grenvillian belts: Amazonia; Laurentia and Baltica (e.g. Dalziel 1992, 1997; Hartz & Torsvik 2002; Tohver *et al.* 2002, 2006b; Meert & Torsvik 2003). Our pole dates from a time when the Grenvillian orogenesis had already peaked, followed by a long period (300–400 Ma) of tectonic quiescence, which ended with the opening of the Iapetus Ocean at the end of Precambrian times (Cawood *et al.* 2001; McCausland *et al.* 2007a).

Palaeomagnetic data have been shown to be consistent with such a connection (Tohver *et al.* 2002; D'Agrella *et al.* 2008); however, with a relative motion between the continents between 1200 and 1150 Ma. Isotopic evidence for Amazonian heritage in blocks of the present-day eastern margin of Laurentia supports this scenario of a mobile connection between these two cratons from *ca*. 1200 to 1150 Ma (e.g. Tohver *et al.* 2004b, 2006a). Because of the ongoing relative motion between the North and South American cratons during the Grenvillian epoch, palaeomagnetic tests must be made by comparison of individual poles for Amazonia and Laurentia for the 1200–980 Ma interval (Fig. 11), instead of comparing the apparent polar wander paths (APWPs) of the two continents. Reconstructions based on this technique are not geometrically unique, but they avoid the assumption of a fixed relative geometry.

The key to these reconstructions is the apparent polar wander for Laurentia between 1250 and 950 Ma. In Table 3, we have compiled a set of high-quality poles ($Q \geq 4$) for Laurentia from 1230 to 1015 Ma. We use these poles to draw the APWP for Laurentia from 1230 to 1050 Ma (Fig. 11a), arranged into a counterclockwise loop (e.g. Meert & Torsvik 2003). For times after 1100 Ma, the APWP for Laurentia becomes more difficult to discern. The controversy arises from the interpretation of the ages of poles obtained on undated sedimentary rocks and from the post-collisional cooling of metamorphic rocks of the Grenville belt which define the path between 1050 and 800 Ma (see discussion in Weil *et al.* 2006). In addition, the younger poles (900–800 Ma) overlap well-defined Late Neoproterozoic–Cambrian poles, and their magnetization may represent a remagnetization (Warnock *et al.* 2000). The Haliburton pole (Buchan & Dunlop 1976), which defines the younger segment of the Mesoproterozoic Laurentia path, has recently been reassessed by Warnock *et al.* (2000), who suggest an age of 1015 ± 15 Myr for the Haliburton thermal remanent magnetization on the basis of thermochronological data. Recently, McCausland *et al.* (2007b) presented a new preliminary palaeomagnetic pole (Plat. = 18.3°N; Plon. = 146.4°E; A_{95} = 6.2) for the 974 ± 6 Ma (U–Pb zircon)

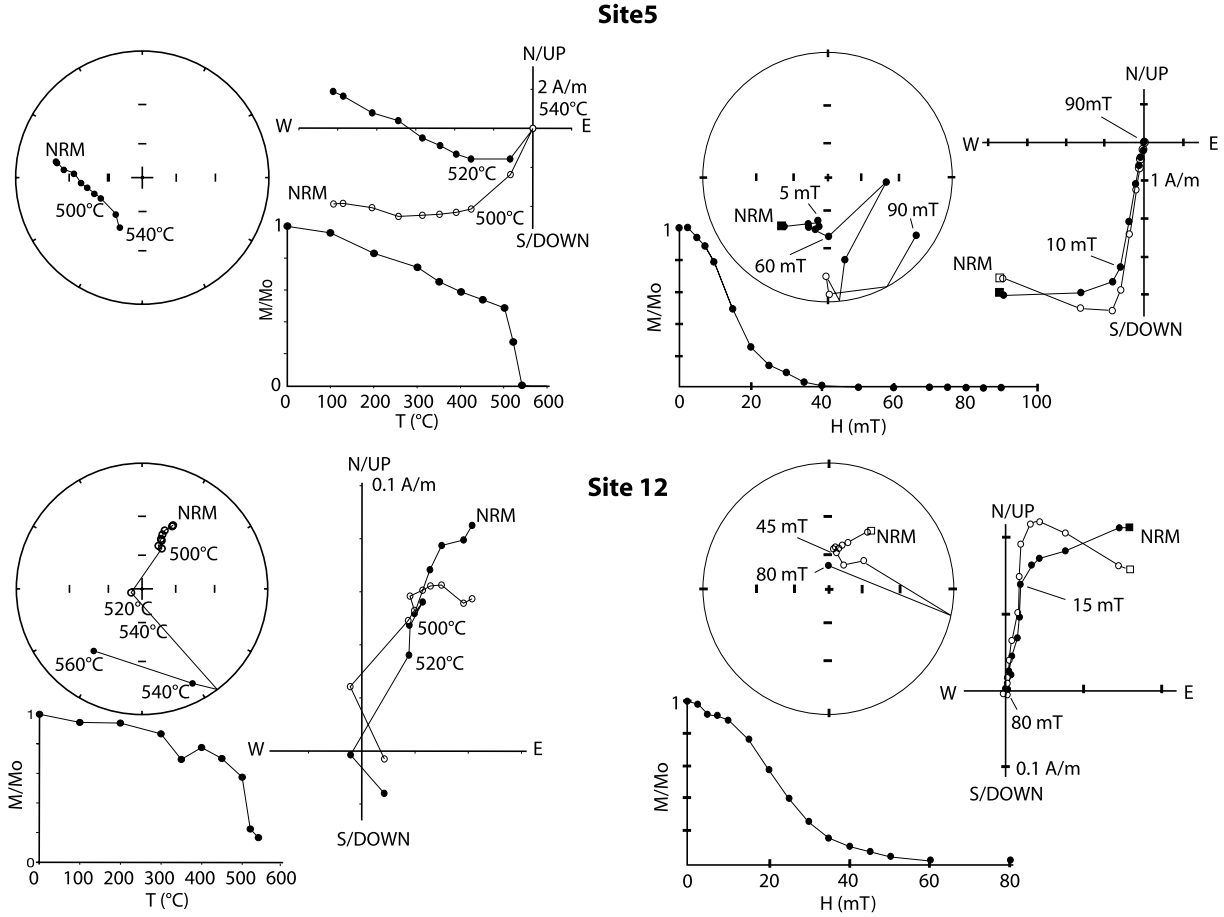

Figure 9. (*Continued*.)

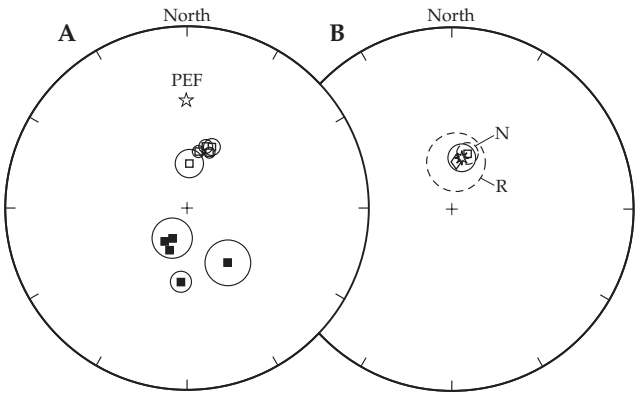

Figure 10. (a) Lower hemisphere equal area stereographic projection plot of site mean remanence directions isolated in the sills together with the 95 per cent cone of confidence. (b) The means of the normal (N, □) and reversed (R, ◇; here with polarity inverted to normal) site means are shown with hatched cones of confidence and the formation mean (✲) is shown with full drawn cone of confidence. Open (closed) symbols denote negative (positive) inclinations. PEF is the expected direction of the present dipole field.

Gilbert Bay dykes, which presents a positive baked contact test. If substantiated, these results constitute the best-defined primary magnetic remanence from Laurentia, preserved in the immediate aftermath of Grenville metamorphism.

The palaeomagnetic reconstruction based on the three poles from Amazonia places Amazonia along the eastern border of Laurentia between 1200 and 980 Ma, using slightly different rotation poles (Table 4). The obtained palaeogeographic configurations is consistent with a continuous relative movement of these two cratons through a large-scale sinistral transcurrent movement (D'Agrella-Filho *et al.* 2008).

In our 980 Ma reconstruction, Amazonia is rotated 63.5° into a position with its northern part attached to eastern Laurentia. This rotation is calculated using the rotation parameters of Table 4, which places the rotated Aguapeí sills pole over the Gilbert Bay pole. Note that the 980 Ma position for Amazonia relative Laurentia is similar to what has been proposed by other authors for the Rodinia reconstruction (e.g. Dalziel 1992, 1997; Torsvik *et al.* 1996; Weil *et al.* 1998; Dalziel *et al.* 2000). This position concludes the scenario of Amazonia moving in a present northeastward direction along the margin of Laurentia from 1200 to 980 Ma, meanwhile rotating counter-clockwise by approximately 180°. Most of this rotation is indicated to have occurred between 1150 and 980 Ma, with a rotation rate of $\sim 1^\circ$ Myr^{-1}. Post-collisional rotations of large plates have been reported elsewhere, for example, from the oblique collision of the Indian plate with Asia (Treloar & Coward 1991). The rotation rate for India was estimated at 0.4°–0.6° Myr^{-1}, that is, the same order of magnitude as suggested here for Amazonia. We may speculate a similar scenario of oblique docking of Amazonia with Laurentia.

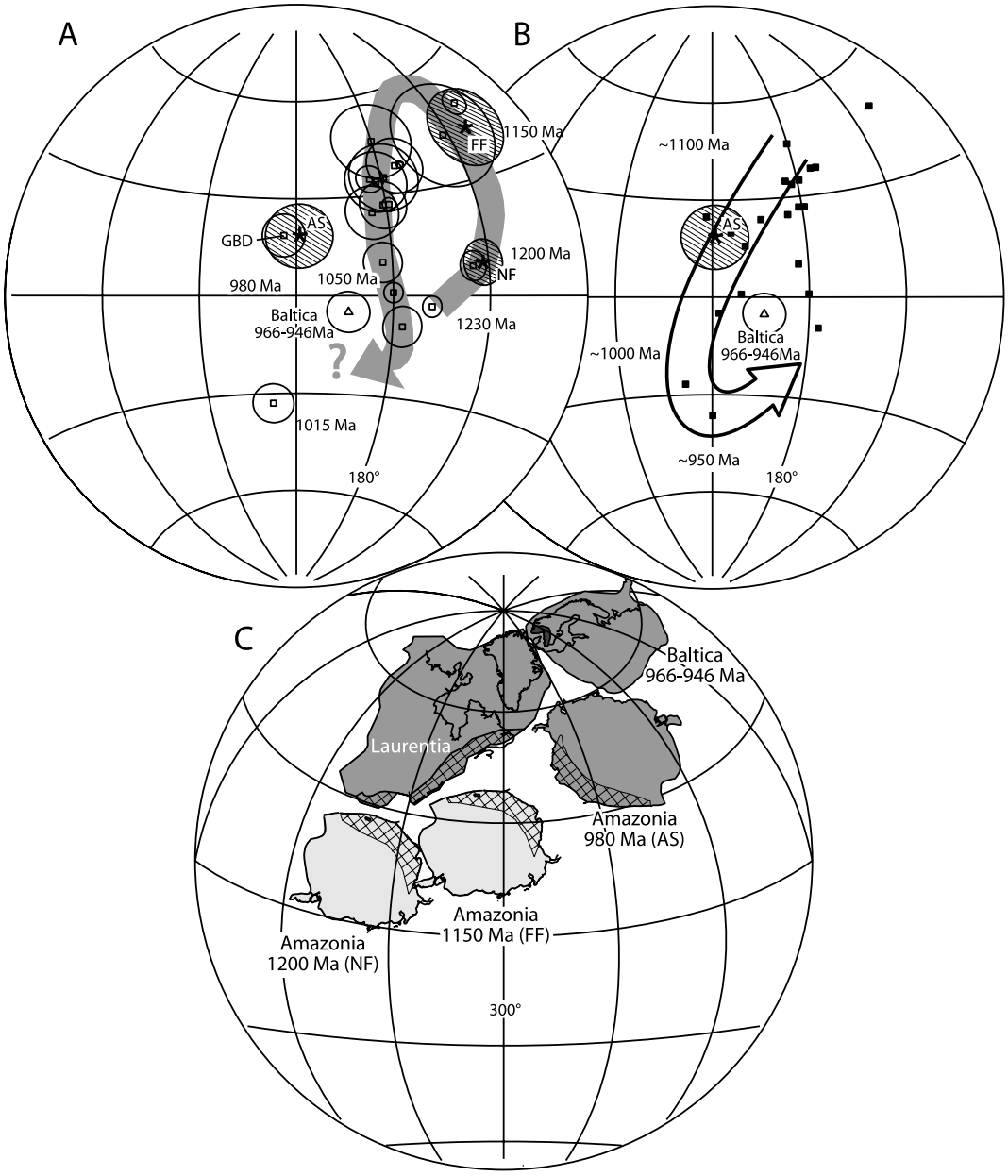

Figure 11. (a) The 1230–1015 Ma apparent polar wander path traced for Laurentia is shown as a shaded loop based on the poles listed in (Table 3. Poles NF, FF and AS (stars) are the Nova Floresta (1200 Ma), Fortuna Formation (1150 Ma) and Aguapeí sills (980 Ma, this work), respectively, from the Amazon Craton rotated according to the rotation parameters presented in (Table 4. Note that the APWP for Laurentia at 1.0–0.95 Ma is poorly defined and not outlined here. (b) After rotation, the AS and the Baltica poles plot in positions similar to what Weil *et al.* (1998, 2006) suggested for a *ca.* 1.10–0.95 Ma segment of the Laurentia APWP, shown here as a large arrowed loop. The black squares are Laurentia poles that range in age from 1113 to 960 Ma and refer to a selection of poles made by Weil *et al.* 1998 (their Table 1). (c) Tectonic reconstruction of the Amazon and Baltica cratons relative to Laurentia. Amazonia and Baltica have been rotated according to the rotation parameters of Table 4. Laurentia is shown in present coordinates. In the reconstruction at 980 Ma (Laurentia, Baltica and Amazonia in dark grey), the position of Baltica is based on a 966–946 Ma mean pole (Table 3), whereas that of Amazonia is from this work. The position of Amazonia at 1150 Ma is from D'Agrella-Filho *et al.* (2008) and at 1200 Ma is from Tohver *et al.* (2002). Rotation parameters are presented in Table 4.

There is mismatch in the geological history between Rondonia and Eastern Bolivia, which suggests the Paraguá Craton and the Arequipa-Antofalla Basement should be regarded as allochtonous with respect to Amazonia (Loewy *et al.* 2004; Boger *et al.* 2005; Cordani *et al.* 2009). Various scenarios for the accretion of these terranes to Amazonia have been presented (e.g. Loewy *et al.* 2004; Boger *et al.* 2005). Ramos (2008) suggested that the Arequipa terrane was trapped during collision between Laurentia and Amazonia in the Mesoproterozoic, and Loewy *et al.* (2004) suggested that the Arequipa-Antofalla Basement collided with Amazonia as part of a larger continent.

If the Paragua Craton and the Arequipa Antofalla Basement separate from Amazonia, amalgamated to Laurentia at 1300–1400 Ma, as may be indicated by the Rondonia–San Ignacio collisional orogeny (e.g. Cordani & Teixeira 2007), which is expressed by several metamorphic belts, large shear zones and recurrent

Table 3. Reference poles for Laurentia, Amazonia and Baltica.

	Age (Ma)	Plat. (°N)	Plong. (°E)	A_{95}(°)	Q	Ref
Laurentia						
Sudbury Dykes	1235	−3	192	3	6	1,2
Upper Bylot	1204	8	205	4	5	3, 4
Abitibi Dykes	1141	43	208	14	6	5, 6
Seabrook Lake carbonatites	1113	46	180	11	6	7
Mean Logan Sills	1109	49	220	3	5	8
Mean Logan dykes	1100	35	181	10	6	8
Lower Normal, Upper Osler Group	1098	34	178	9	4	9
Portage Lake Volcanics	1095	27	181	2	4	10
Mamainse Point Volcanics	1090	38	188	1	4	11
Chipman Lake Carbonatites	1090	38	186	8	5	7
Clay-Howells Carbonatite Complex	1075	27	179	7	5	12
Michipicoten Island Volcanics	1075	25	175	8	4	11
Copper Harbor Conglomerate	1060	35	176	4	5	13
Nonesuch Shale	1046	10	177	6	5	14
Freda Sandstone	1030	1	180	3	4	14
Jacobsville Sandstone	1020	−9	183	6	5	15
Halliburton Intrusions	1015	−33	142	6	4	16, 17
Gilbert Bay Dykes	975	18	146	6	6	18
Amazonia						
Nova Floresta Formation	1200	−25	345	6	5	19
Fortuna Formation	1150	−60	336	10	5	20
Aguapeí Sills	980	−64	271	9	5	This work
Baltica						
Nilstorp*	966	9	239	8	3	21
Dala dolerites*	946	5	239	13	4	22
Karlshamn-Fäjö*	946–954	2	242	30	4	23
Mean *	946–966	5	240	6	5	This work

Note: 1, Schwarz & Buchan (1982); 2, Dudas *et al.* (1994); 3, Fahrig *et al.* (1981); 4, Kah *et al.* (2001); 5, Ernst & Buchan (1993); 6, Krogh *et al.* (1987); 7, Symons (1992); 8, Halls & Pesonen (1982); 9, Halls (1974); 10, Books (1972); 11, Palmer & Davis (1987); 12, Lewchuk & Symons (1990); 13, Halls & Palmer (1981); 14, Henry *et al.* (1977); 15, Roy & Robertson (1978); 16, Hyodo & Dunlop (1993); 17, Warnock *et al.* (2000); 18, McCausland *et al.* 2007b; 19,Tohver *et al.* (2002); 20, D'Agrella-Filho *et al.* (2008); 21, Patchett & Bylund (1977) and Söderlund *et al.* 2004; 22, Bylund (1992) and Söderlund *et al.* (2005); 23, Patchett & Bylund (1977) and Söderlund *et al.* (2004).
The symbol * denotes the palaeomagnetic data for Baltica included in the mean calculation.
Q denotes quality index (Van der Voo 1990).

Table 4. Palaeomagnetic poles and rotation parameters used in the reconstruction of Fig. 11.

Palaeomagnetic poles and rotated poles for Amazonia and Baltica									
		Rotation parameters			Pole		Rotated pole		
Pole	Age (Ma)	Plat. (°N)	Plon. (°E)	θ°	Plat. (°N)	Plon. (°E)	Plat. (°N)	Plon. (°E)	Ref.
NF	1200	8.7	280.2	−156.5	−25	345	9	208	1
FF	1150	10.5	298.7	−150.0	−60	336	43	218	2
AS	980	40.4	224.1	63.5	−65	281	18	151	This work
Baltica	946 – 966	66.3	41.3	−78.2	5	240	–4	167	This work
Laurentian poles in present coordinate system									
UB	1204						8	205	3,4
AD	1141						43	208	5,6
GBD	974						18	146	7

Note: NF, Nova Floreste pole; FF, Fortuna Formation pole; AS, Aguapeí Sills, Baltica-mean 946–966 Ma; UB, Upper Bylot; AD, Abitibi Dykes; GBD, Gilbert Bay Dykes.
1, Tohver *et al.* (2002); 2, D'Agrella-Filho *et al.* (2008); 3, Fahrig *et al.* (1981); 4, Kah *et al.* (2001); 5, Ernst & Buchan (1993); 6, Krogh *et al.* (1987) and McCausland *et al.* 2007b.

plutonism and magmatic arcs of similar ages in southern Laurentia (Van Schmus *et al.* 1996), Amazonia would have docked obliquely to Laurentia at *ca*. 1200 Ma. This initiated the transcurrent movement, which lasted until the collision with the Paragua craton (Tohver *et al.* 2004a, 2006a) and the Arequipa Antofalla Basement, at 1150–1100 Ma, manifested by the sinistral Ji–Parana shear zone (Tohver *et al.* 2005a) and the metamorphism in the Nova Brasilandia (NB) belt (Tohver *et al.* 2004a, 2005a). The oblique docking and this collision could be the reason for the rotation of Amazonia as indicated here.

It shall be pointed out that our high-quality pole for Amazonia at 980 Ma is not matched by similarly well-defined poles for Laurentia for the same age, which makes our tectonic reconstruction versus Laurentia tentative.

A palaeogeographic position of Baltica relative Laurentia at *ca*. 1.0 Ga can be calculated using a 966–946 Ma mean pole for Baltica (Table 3). After a rotation of –78.2° around an Euler pole (66.3°N, 41.3°E), the rotated pole falls between the 1020 Ma Jacobsville sandstone pole and the rotated Aguapei sills pole (Fig. 11). This rotation places Baltica north of the Amazon craton, and the data are compatible with an attachment of Baltica to the northeastern part of Laurentia (Greenland). A similar position for Baltica in Rodinia reconstructions has been suggested by many authors (e.g. Torsvik *et al.* 1996; Dalziel 1997). Such a relative position of Baltica and Laurentia is supported by a 950–930 Ma metamorphic event in central East Greenland (Watt & Thrane 2001), which is contemporaneous with high grade metamorphism in the Sveconorwegian orogenic belt in the southwestern part of Baltica (Johansson & Larionov 1999; Möller 1999). Note, however, that this part of Baltica is in our reconstruction located north of central East Greenland. Provenance studies from detrital zircon analyses made by Watt & Thrane (2001) suggest that the metamorphosed sediments in East Greenland have a Laurentian–Amazonian affinity. This supports the tectonic reconstruction presented here, with a close link between Amazonia, Laurentia and Baltica at *ca*. 980 Ma. The relative position of Amazonia, Laurentia and Baltica at this time is similar to the Rodinia configuration proposed by Li *et al.* (2008); however, the orientation of Amazonia is significantly different.

There is little evidence for a Grenville-age collision in northern Amazonia and southern-southwestern Baltica. Keppie & Ortega-Gutierrez (1999) suggest that two Central American blocks, the Oaxaquia and Chortis, originated as arcs in a Grenvillian ocean between Laurentia, Baltica and Amazonia. The high-grade collisional metamorphism in these blocks is proposed to be the result of the collisions with Laurentia, Baltica and Amazonia at *ca*. 1000 Ma, and in Rodinia reconstructions (Pisarevsky *et al.* 2003; Li *et al.* 2008), the Oaxaquia block is placed along the northern margin of Amazonia, within the zone of collision with Baltica. This position of the Oaxaquia block is consistent with palaeomagnetic data (Ballard *et al.* 1989), and Pisarevsky *et al.* (2003) presented a scenario where the Oaxaquia and the Chortis blocks may represent a continental arc formed on the present northern margin of Amazonia. Evidence for a Late Neoproterozoic link between Laurentia, Baltica and Amazonia (Pisarevsky *et al.* 2008 and references therein) suggests that the Rodinia configuration of these continents (Li *et al.* 2008) lasted until 610–550 Ma. This is indicated by coeval rift related mafic magmatism along the eastern margin of Laurentia and the western and southwestern margin of Baltica and mafic magmatism of this age (546 Ma) in Oaxaquia (Keppie *et al.* 2006). The Oaxaquia block is, in the reconstruction by Pisarevsky *et al.* (2008), located close to a volcanic province of similar age in western Ukraine (e.g. Elming *et al.* 2007).

The West African Craton is often proposed to be associated with the northeastern margin of Amazonia during the Late Precambrian (e.g. Trompette 1997; Cordani *et al.* 2003). The Gondwanaland Amazonia–West African fit has also been used in the Rodinia reconstructions (e.g Li *et al.* 2008). However, there is no reliable palaeomagnetic data available to verify that. A Gondwanaland fit with West Africa is not consistent with our reconstruction at 980 Ma, with Baltica located close to the present northeastern part of Amazonia.

CONCLUSION

A Late Mesoproterozoic palaeomagnetic pole for the Amazon craton is calculated from primary remanent magnetizations of basic sills in the southwestern part of the craton. The primary origin is demonstrated by a dual polarity in these unmetamorphosed rocks, and AMS data suggest that the sills and dykes are in their original position. The $^{40}Ar/^{39}Ar$ analyses revealed a well-defined plateau age at 981 $\pm$ 2 Myr for one site of the sill complex and indicate that some of the dykes are older than the sills.

On the basis of the pole to pole reconstruction presented here and geological data suggesting sinistral strike-slip shear in southwestern Amazonia in the time interval 1200–1100 Ma, we propose a scenario where Amazonia collided with Laurentia at *ca*. 1200 Ma and moved northeastwards along the present southeast coast of Laurentia and, meanwhile, rotated counter-clockwise by approximately 180°. At *ca*. 980 Ma, the palaeomagnetic data is consistent with northern–northwestern part of Amazonia attached to eastern Laurentia (Greenland), and the northeastern margin of Amazonia was facing the southern margin of Baltica, with the Oaxaquia block possibly in between. In this geometry for Rodinia, representing the end of Grenvillian orogenesis, the position of Amazonia is similar to the position in other models of Rodinia; however, the orientation is significantly different.

Since the high-quality pole for Amazonia at 980 Ma is not matched by similarly well-defined poles for Laurentia for the same age, our tectonic reconstruction is tentative. New palaeomagnetic data from well-dated 1000–950 Ma rocks from Laurentia are needed to further test the scenario presented here.

ACKNOWLEDGMENTS

This work was financially supported by grants from FAPESP (grants 03/12802–2 and 07/59531), CNPq (grant 55.4458/05–5) and the Swedish Research Council (grant 2002–4886). The authors are greatful to Phil McCausland and an anonymous reviewer for their comments, which greatly improved the quality of this manuscript.

REFERENCES

Annells, R.N., Fletcher, C.J.N., Burton, C.C.J. & Evans, R.B., 1986. *The Rincon del Tigre Igneous Complex: a major layered Ultra-mafic intusion of Proterozoic age in the Precambrian shield of eastern Bolivia. Part I: geology and mineral potential,* pp. 1–24, Overseas Geology and Mineral Resources No. 63, Brit. Geol. Surv., Keyworth.

Ballard, M.M., Van Der Voo, R. & Urrutia-Fucugauchi, J., 1989. Paleomagnetic results from Grenvillian-aged rocks from Oaxaca, Mexico: evidence for a displaced terrane, *Precambrian Res.,* **42,** 343–352.

Barros, A.M. *et al*., 1982. Geologia, in *Projecto RADAMBRASIL, Folha SD. 21. Cuiabá,* Ministério das Minas e Energia Rio de Janeiro, pp. 544.

Bettencourt, J.S., Tosdal, R.M., Leite Junior, W.B. & Payola, B.L., 1999. Mesoproterozoic rapakivi granites of Rondonia Tin Province, southwestern border of the Amazonian craton, Brazil, I: reconnaissance U–Pb geochronology and regional implications, *Precambrian Res.*, **95,** 41–67.

Boger, S.D., Raetz, M., Giles, D., Etchart, E. & Fanning, C.M., 2005. U-Pb age data from the Sunsas region of Eastern Bolovia, evidence the allochthonous origin of the Paragua block, *Precambrian Res.,* **139,** 121–146.

Books, K.G., 1972. Paleomagnetism of some Lake Superior Keweenawan rocks, *U.S. Geol. Surv. Prof. Pap.* **760,** 42.

Buchan, K.L. & Dunlop, D.J, 1976. Paleomagnetism of the Haliburton intrusions: superimposed magnetizations, metamorphism, and tectonics in the late Precambrian, *J. geophys. Res.,* **81,** 2951–2967.

Buchan, K.L., Ernst, R.E., Hamilton, M.A., Mertanen, S., Pesonen, L.J. & Elming, S.-Å., 2001. Rodinia: the evidence from integrated palaeomagnetism and U-Pb geochronology, *Precambrian Res.,* **110,** 9–32.

Bylund, G., 1992. Palaeomagnetism, mafic dykes and the Protogine Zone, southern Sweden, *Tectonophysics,* **201,** 49–63.

Cawood, P.A., McCausland, P.J.A., Dunning, G.R., 2001. Opening Iapetus: Constraints from the Laurentian margin in Newfoundland, *Geol.. Soc. Am. Bull.,* **113,** 443–453.

Cordani, U.G. & Teixeira, W., 2007. Proterozoic accretionary belts in the Amazonian Craton, *in4-D Framework of Continental Crust,* Vol. 200, pp. 297–320, eds Hatcher, R.D. jr, Carlson, M.P., McBride, J.H. & Martinez-Catalán, J.R. (Org.), *USA: Geological Society of America,* Denver.

Cordani, U.G., Brito-Neves, B.B., D'Agrella-Filho, M.S.D., 2003. From Rodinia to Gondwana: a review of the available evidence from South America, *Gondwana Res.,* **6**(2), 275–283.

Cordani, U.G., Teixeira, W., D'Agrilla-Filho, M.S. & Trinidade, R.J., 2009. The position of the Amazonian Craton in the Supercontinents, *Gondwana Res.,* in press.

D'Agrella-Filho, M.S., Trinidade, R.I.F., Siquiera, R., Ponte-Neto, C.F. & Pacca, I., 1998. Paleomagnetic constraints on the Rodinia supercontinent: implications for its Neoproterozoic break-up and the formation of Gondwana, *Int. Geol. Rev.,* **40,** 171–188.

D'Agrella-Filho, M.S., Tohver, E., Santos, J.O.S., Elming, S.-A., Trindade, R.I.F., Pacca, I.I.G. & Geraldes, M.C., 2008. Direct dating of paleomagnetic results from Precambrian sediments in the Amazon craton: evidence for Grenvillian emplacement of exotic crust in SE Appalachians of North America, *Earth planet. Sci. Lett.,* **267,** 188–199.

Dalrymple, G.B. & Lanphere, M.A., 1971. $^{40}Ar/^{39}Ar$ technique of K-Ar dating: a comparison with the conventional technique, *Earth planet. Sci, Lett.,* **12,** 300–308.

Dalziel, I.W.D., 1991. Pacific margins of Laurentia and east Antartica-Australia as a conjugate rift pair: evidence and implications, *Geology,* **19,** 598–601.

Dalziel, I.W.D., 1992. On the organization of the American plates in the Neoproterozoic and the breakout of Laurentia, *GSA Today,* **2**(2), 237–141.

Dalziel, I.W.D., 1997. Neoproterozoic-Paleozoic geography and tectonics: review, hypothesis, environmental speculations, *GSA Bull.,* **109,** 16–42.

Dalziel, I.W.D., Mosher, S. & Gahagan, L.M., 2000. Laurentia-Kalahari collision and the assembly of Rodinia, *J. Geol.,* **108,** 499–513.

Day, R., Fuller, M.D., Schmidt, V.A.,1977. Hysteresis properties of titanomagnetites: grain size and composition dependence, *Phys. Earth planet. Inter.,* **13,** 260–267.

Dudas, F.O., Davidson, A. & Bethune, K.M., 1994. Age of the Sudbury diabase dyke and their metamorphism in the Grenvillian Province, Ontario, in *Radiogenic age and isotopic studies,* Report No. 8, Geol. Surv. Can., *Curr. Res.*, **1994F**, pp. 97–106.

Dunlop, D.J. & Özdemir, Ö., 1997. *Rock Magnetism, Fundamentals and Frontiers,* Cambridge University Press, Cambridge, 573 pp.

Elming, S.-Å., & Mattsson, H., 2001. Post Jotnian basic dykes in the Fennoscandian Shield and the break up of Baltica from Laurentia: a palaeomagnetic and AMS study, *Precambrian Res.,* **108,** 215–236.

Elming, S.-Å., Kravchenko, S., Layer, P., Rusakov, O.M., Glevasskaya, A.M., Mikhailova, N.P. & Bachtadse, V., 2007. Palaeomagnetism and $^{40}Ar/^{39}Ar$ age determinations of the Ediacaran traps from the southwestern margin of the East European Craton, Ukraine: relevance to the Rodinia break-up, *J. Geol. Soc. Lond.,* **164,** 969–982.

Ernst, R.E. & Buchan, K.L., 1993. Paleomagnetism of the Abitibi dike swarm, southern Superior Province, and implications for the Logan Loop. *Can. J. Earth Sci.* **30,** 1886–1897.

Fahrig, W.F., Christie, K.W. & Jones, D.L., 1981. *Paleomagnetism of the Bylot basins; Evidence for Mackenzie Continental Tensional Tectonics,* Paper 81–10, Geol. Survey of Canada, pp. 303–312.

Fisher, R.A., 1953. Dispersion on a sphere, *Proc. R. Soc. Lond. A,* **217,** 295–305.

Geraldes, M.C., Van Schmus, W.R., Condie, K.C., Bell, S., Teixeira, W., Babinski, M., Bartly, J.K. & Kah, L.C., 2001. Proterozoic geological evolution of the SW part of the Amazonian craton in Mato Grosso State, Brazil, *Precambrian Res.,* **111,** 91–128.

Geraldes, M.C., Teixeira, W. & Heilbron, M., 2004. Lithospheric versus asthenospheric source of the SW Amazonian craton A-types granites: the role of the Paleo and Mesoproterozoic accretionary belts for their coeval continental suites, *Episodes,* **25,** 3, 185–189.

Halls, H.C., 1974. A paleomagnetic reversal in the Oster volcanic group, Northern Lake Superior, *Can. J. Earth Sci.,* **11,** 1200–1207.

Halls, H.C. & Palmer, H.C., 1981. Remagnetization in Keweenawan rocks Part II. Lava flows within the Copper Harbor conglomerate, Michigan, *Can. J. Earth Sci.,* **18,** 1395–1408.

Halls, H. & Pesonen, L., 1982. Paleomagnetism of Kewenawan rocks, in *Geology and Tectonics of the Lake Superior Basin,* Vol. 156, pp. 173–201, eds Wold, R.J. & Hinze, W.J., *Geol. Soc. Am. Mem*.

Hargraves, R.B., 1968. Paleomagnetism of the Roraima dolerites, *Geophys. J. R. astro. Soc.,* **16,** 147–160.

Hartz, E.H. & Torsvik, T.H., 2002. Baltica upside down: a new plate tectonic model for Rodinia and the Iapetus Ocean, *Geology,* **30,** 255–258.

Henry, S.G., Mauk, F.J. & Van Der Voo, R., 1977. Paleomagnetism of the upper Kewenawan sediments: the Nonesuch shale and the Freda sandstone, *Can. J. Earth Sci.,* **14,** 1128–1138.

Hoffman, P.F., 1991. Did the breakout of Laurentia turn Gondwana inside out? *Science,* **252,** 1409–1412.

Hrouda, F., 1982. Magnetic anisotropy of rocks and its application in geology and geophysics. *Geophys. Surv.,* **5,** 37–82.

Hyodo, H. & Dunlop, D.J., 1993. Effect of anisotropy on the paleomagnetic contact test for a Grenvillian dyke, *J. geophys. Res.,* **98,** 7997–8017.

Jelinek, V., 1978. Statistical processing of anisotropy of magnetic susceptibility measured on groups of specimens, *Studia Geophysica et Geodetica,* **22,** 50–62.

Jelinek, V., 1981. Characterisation of the magnetic fabric of rocks, *Tectonophysics,* **79,** 63–67.

Johansson, A. & Larionov, A., 1999. Late palaeoproterozoic, Grenvillian and Caledonian magmatism on eastern Svalbard, in *Proceedings of the Second Symposium on East Greenland Geology, Mainly Caledonian,* Rapport 1999/21, pp. 45–46, eds Fredriksen, K.S. & Thrane, K., Danmarks og Grönlands Geologiske Undersökelse.

Kah, L.C., Lyons, T.W. & Chesley, J.T., 2001. Geochemistry of a 1.2 Ga carbonate-evaporate succession, northern Baffin and Bylot Islands: implications for Mesoproterozoic marine evolution, *Precambrian Res.,* **111,** 203–234.

Keppie, J.D. & Ortega-Gutierres, F.O., 1999. Middle American Precambrian basement: a missing piece of the reconstructed 1-Ga orogen, in *Laurentia-Gondwana connections before Pangea,* Vol. 336, pp. 199–210, Geological Society of America Special Paper.

Keppie, J.D., Dostal, J., nance, R.D., Miller, B.V., Ortega-Gutierres, A. & Lee, J.K.W., 2006. Circa 546 Ma plume-related dykes in the c. 1 Ga Novillo Gneiss (east-central Mexico): evidence for the initial separation of Avalonia, *Precambrian Res.,* **147,** 342–353.

Kirschvink, J.L., 1980. The least – squares line and plane and the analysis of palaeomagnetic data, *Geophys. J. R. astr. Soc.,* **62,** 699–718.

Knight, M.D. & Walker, G.P.L., 1988. Magma flow directions in dikes of the Koolau Complex, Oahu, determined from magnetic fabric studies. *J. geophys. Res.* **93,** 4301–4319.

Krogh, T.E. *et al*., 1987. Precise U-Pb ages of diabase dykes and mafic to ultra-mafic rocks using trace amounts of baddeleyite and zircon, in *Mafic Dyke Swarms,* Vol. 34, pp. 147–152, eds Halls, H.C. & Fahrig, W.F., Geol. Ass. Can. Spec. Pap.

Lewchuk, M.T. & Symons, D.T.A., 1990. Paleomagnetism of the Clay–Howells carbonatite complex: constraints on Proterozoic motion in the Kapuskasing Structural Zone, Superior Province, Canada, *Tectonophysics,* **172,** 67–75.

Li, Z.X. *et al*., 2008. Assembly, configuration, and break-up history of Rodinia: a synthesis, *Precambrian Res.,* **160,** 179–210.

Litherland, M. *et al*., 1989. The Proterozoic of Eastern Bolivia and its relationship to the Andean Mobile Belt, *Precambrian Res.,* **43,** 157–174.

Loewy, S.L., Connelly, J.N., Dalziel, I.W.D., 2004. An orphaned basement block: the Arequipa-Antofalla Basement of the central Andean margin of South America, *Geol. Soc. Am. Bull.,* **116,** 171–187.

McCausland, P.J.A., Van Der Voo, R. & Hall, C.M., 2007a. Circum – Iapetus Paleogeography of the Precambrian-Cambrian transition with a new paleomagnetic constraint from Laurentia, *Precambrian Res.,* **156,** 125–152.

McCausland, P.J.A., Gower, C., Hodych, J.P., Pazold, R. & Turbett, M., 2007b. A new Laurentian paleopole from the 974 Ma Gilbert Bay dykes, southeastern Labrador (Abstract), in *Recent advances in the geology of Laurentia*, Technical program No. SS3, Geological Association of Canada, Structural Geology and Tectonic Division, Yellowknife,.

McFadden, P.L. & Lowes, F.J., 1981. The discrimination of mean directions drawn from Fisher distributions, *Geophys. J. R. astr. Soc.,* **67,** 19–33.

McMenamin, M.A.S. & McMenamin, D.L., 1990. *The Emergence of Animals: The Cambrian Breakthrough,* Columbia University Press, New York, 217 pp.

Meert, J.G. & Torsvik, T.H., 2003. The making and unmaking of a supercontinent: Rodinia revisited. *Tectonophysics,* **375,** 261–288.

Meert, J.G. & Lieberman, B.S., 2004. A palaeomagnetic and palaeobiogeographical perspective on latest Neoproterozoic and early Cambrian tectonic events. *J. Geol. Soc. Lond.,* **161,** 477–487.

Möller, C., 1999. Sapphirine in SW Sweden: a record of Sveconorwegian (-Grenvillian) late-orogenic tectonic exhumation. *J. Metamorphic Geol.,* **17,** 127–141.

Onstott, T.C., Hargraves, R.B., Cork, D., & Hall, C., 1984. Constraints on the motion of South American and African shields during the Proterozoic. I. $^{40}Ar/^{39}Ar$ and paleomagnetic correlations between Venezuela and Liberia. *Geol.. Soc. Am. Bull.,* **95,** 1045–1054.

Palmer, H.C. & Davis, D.W., 1987. Paleomagnetism and U-Pb geochronology of volcanic rocks from Michipicoten Island, Lake Superior, Canada: precise calibration of the Keweenawan polar wander track, *Precambrian Res.,* **37,** 157–171.

Patchett, P.J. & Bylund, G., 1977. Age of Grenville Belt magnetization: Rb-Sr and paleomagnetic evidence from Swedish dolerites, *Earth planet. Sci. Lett.,* **35,** 92–104.

Pesonen, L.J. *et al*, 2003. Palaeomagnetic configuration of continents during the Proterozoic. *Tectonophysics,* **375,** 289–324.

Piper, J.D.A., 1976. Palaeomagnetic evidence for a Proterozoic supercontinent. *Phil. Trans. R. Soc. Lond., A* **280,** 469–490.

Pisarevsky, S.A., Wingate, M.T.D., Powell, C., Jonson, S., & Evans, D.A.D., 2003. Models of Rodinia assembly and fragmentation, in *Proterozoic East Gondwana: Supercontinent Assembly and Breakup,* Vol. 206, pp. 35–55, eds Yosida, M., Windley, B.F. & Dasgupta, S., Geol. Soc. Spec. Publ.

Pisarevsky, S.A., Murphy, J.B., Cawood, P.A. & Collins, A.S., 2008. Late Neoproterozoic and Early Cambrian palaeogeography: models and problems, in *West Gondwana: Pre-Cenozoic Correlations Across the South Atlantic Region,* Vol. 294, pp. 9–31, eds Pankhurst, R.J., Trouw, R.A.J., Brito Neves, B.B. and De Wit, M.J., Geol.. Soc. London Spec. Publ.

Priem, H.N.A., Bon, E.H., Verdurmen, E.A.Th. & Bettencourt, J.S., 1989. Rb-Sr geochronology of Precambrian crustal evolution in Rondinia (western margin of the Amazonian craton), *Brazil. J. S. Am. Earth Sci.,* **2,** 163–170.

Ramos, V.A., 2008. The basement of the Central Andes: the Arequipa and related terranes. *Ann. Rev. Earth planet Sci.,* **36,** 289–324.

Renne, P.R., Swisher, C.C., Deino, A.L., Karner, D.B., Owena, T.L. & DePaolo, D.J., 1998. Intercalibration of standards, absolute ages and uncertainties in $^{40}Ar/^{39}Ar$ dating, *Chem. Geol.,* **145,** 117–152.

Rizzotto, G.J., Lima, E.F., Chemale Junior, F., 2001. Geologia do Grupo Nova Brasilandia, sudeste de Rondonia, acrecao continental e implicacoes geotectonica, in *Contribuicoes à Geologia da Amazonia,* Vol. 2, pp. 342–442, coordinators Reis, N.J. & Monteiro M.A.S., SBG.

Roy, J.L. & Robertson, W.A., 1978. Paleomagnetism of the Jabobsville Formation and the apparent polar path for the interval ∼1100 to ∼670 Ma for North America, *J. geophys. Res.,* **83,** 1289–1304.

Ruiz, A.S., 1992. Contribuicão à geologia do Distrito de Cachoeirinha, MT, *Master thesis*. IG-USP, São Paulo, 98 pp.

Ruiz, A.S., 2005. Evolucão Geológica do Sudeste do Cráton Amazônico, Região Limitrofe Brazil Bolivia—Mato Grosso (Unpublished), *PhD thesis*. Rio Claro, São Paulo, Brazil, pp. 258.

Sadowski, G.R. & Bettencourt, J.S., 1996. Mesoproterozoic tectonic correlations between eastern Laurentia and the western border of the Amazon Craton, *Precambrian Res.,* **76,** 213–227.

Saes, G.S., 1999, Tectonic and paleogeographic evolution of the Aguapeí aulacogen (1.2 – 1.0 Ga) and the basement terranes in the southern Amazon craton, *PhD thesis*. Univ. de São Paulo, São Paulo, 135 pp.

Saes, G.S. & Leite, J.D., 1993. Evolução tectono-sedimentar do Grupo Aguapeí, Proterozoico Medio na porção meridional do craton Amazônico: Mato Grosso e Oriente Boliviano, *Revista Brasileira de Geociências,* **23,** 31–37.

Santos, J.O.S., 2003. Geotectonica dos Escudos das Guianas e Brazil Central, in *Geologia,* pp. 169–226, organizers Bizzi, L.A., Schobbenhaus, C., Vidotti, R.M. & Goncalves, J.H., Tectonica e Recursos Minerais do Brazil, CPRM, Brazila.

Schwarz, E.J. & Buchan, K., 1982. Uplift deduced from remanent magnetization: Sudbury area since 1250 Ma ago, *Earth planet. Sci. Lett.,* **58,** 65–74.

Söderlund, U., Patchett, P.J., Vervoort, J.D. & Isachsen, C.E., 2004. The ^{176}Lu decay constant determined by Lu-Hf and U-Pb isotope systematics of Precambrian mafic intrusions, *Earth planet. Sci. Lett.,* **219,** 311–324.

Söderlund, U., Isachsen, C.E., Bylund, G., Heaman, L.M., Patchett, P.J., Vervoort, J.D. & Andersson, U.B., 2005. U–Pb baddeleyite ages and Hf, Nd isotope chemistry constraining repeated magmatism in the Fennoscandian Shield from 1.6 to 0.9 Ga, *Contrib. Mineral. Petrol.,* **150,** 174–194.

Symons, D.T.A.,1992. Paleomagnetism of the Keweenawan Chipman Lake and Seabrook Lake carbonatite complexes, Ontário, *Can. J. Earth Sci.,* **29,** 1215–1223.

Souza, A.E.P. & Hildred, P.R.,1980. Contribucãao estudo da geologia do Grupo Aguapeí, Mato Grosso, *31 Congr. Bras. De Geol.,* **2,** 587–598.

Tauxe, L., Gee, J.S. & Staudigel, H., 1998. Flow directions in dikes from anisotropy of magnetic susceptibility data: the bootstrap way, *J. geophys. Res.,* **103,** 17 775–17 790.

Tohver, E., Van Der Pluijm, B.A., Van Der Voo, R., Rizzotto, G. & Scandolara, J.E., 2002. Paleogeography of the Amazon craton at 1.2 Ga: Early Grenvillian collision with the Llano segment of Laurentia, *Earth planet. Sci. Lett.,* **199,** 185–200.

Tohver, E., Van Der Pluijm, B.A., Mezger, K., Scandolara, J.E. & Essene, E.J., 2004a. Significance of the Nova Brasilândia Metasedimentary Belt in western Brazil: Redefining the Mesoproterozoic boundary of the Amazon craton, *Tectonics,* **v.23,** TC6004, doi:10.1029/2003TC001563.

Tohver, E., Bettencourt, J.S., Tosdal, R., Mezger, K., Leite, W.B., & Payolla, B.L., 2004b. Terrane transfer during the Grenville orogeny: tracing the Amazonian ancestry of southern Appalachian basement through Pb and Nd isotopes, *Earth planet. Sci. Lett.,* **228,** 161–176. doi:10.1016/j.epsl.2004.09.029

Tohver, E., Van Der Pluijm, B.A., Mezger, K., Scandolara, J.E., & Essene, E.J., 2005a, Two stage tectonic history of the SW Amazon craton in the late Mesoproterozoic: Identifying a cryptic suture zone, *Precambrian Res.*, **137,** 35–59.

Tohver, E., Van Der Pluijm, B.A., Scandolâra, J.E., & Essene, E.J., 2005b, Late Mesoproterozoic deformation of SW Amazonia (Rondônia, Brazil): geochronological and structural evidence for collision with Southern Laurentia, *J. Geol.,* **113,** 309–323.

Tohver, E., Teixeira, W., Van Der Pluijm, B.A., Geraldes, M.C., Bettencourt, J.S., & Rizzotto, G., 2006a. Restored transect across the exhumed Grenville orogen of Laurentia and Amazonia, with implications for crustal architecture, *Geology,* **34**(8), 669–672, doi:10.1130/G22534.1.

Tohver, E., D'Agrella-Filho, M.S., & Trinidade, I.F., 2006b. Paleomagnetic Record of Africa and South America for the 1200–500 Ma interval, and evaluation of Rodinia and Gondwana assemblies, *Precambrian Res.,* **147,** 193–222.

Torsvik, T.H., Smethurst, M.A., Meert, J.G., Van Der Voo, R., McKerrow, W.S., Brasier, M.D., Sturt, B.A. & Walderhaug, H.J., 1996. Continental break-up and collision in the Neoproterozoic and Palaeozoic—a tale of Baltica and Laurentia, *Earth Sci. Rev.,* **40,** 229–258.

Treloar, P.J. & Coward, M.P., 1991. Indian Plate motion and shape: constraints on the geometry of the Himalayan orogen, *Tectonophysics,* **191,** 189–198.

Trompette, R., 1997. Neoproterozoic (∼600 Ma) aggregation of Western Gondwana: a tentative scenario. *Precambrian Res.,* **82,** 101–112.

Van Der Voo, R., 1990. The reliability of paleomagnetic data, *Tectonophysics,* **184,** 1–9.

Van Schmus, W.R., Bickford, M.E. & Turek, A., 1996. Proterozoic geology of the east-central mid-continent basement. in *Basement and basins of eastern North America,* Vol. 308, pp.7–32, eds Van der Pluijm, B.A. & Catacosinos, P.A., Geol.. Soc. Am. Spec. Pap.

Warnock, A.C., Kodama, K.P. & Zeitler, P.K., 2000. Using thermochronometry and low-temperature demagnetization to accurately date Precambrian paleomagnetic poles. *J. geophys. Res.,* **105**(B8), 19 435—19-453.

Watt, G.R. & Thrane, K., 2001. Early Neoproterozoic events in East Greenland, *Precambrian Res.* **110,** 165–184.

Weil, A.B., Van Der Voo, R., Mac Niocaill, C. & Meert, J.G., 1998.The Proterozoic supercontinent Rodinia: paleomagnetically derived reconstructions for 1100 to 800 Ma, *Earth planet. Sci. Lett.,* **154,** 13–24.

Weil, A.B., Geissman, J.W. & Ashby, J.M, 2006. A new paleomagnetic pole for the Neoproterozoic Uinta Mountain supergroup, Central Rocky Mountain Status, USA, *Precambrian Res.,* **147,** 234–259.

Wijbrans, J.R., Pringle, M.S., Koppers, A.A.P. & Scheveers, R., 1995. Argon geochronology of small samples using the Vulkaan argon laserprobe, *Proc. Koninklijke Nederlandse Akademie van Wetenschappen,* **98,** 185–218.

Zijderveld, J.D.A., 1967. A.C. demagnetization of rocks: analysis of results, in *Methods in Palaeomagnetism,* pp. 254–286, eds Collinson, D.W., Creer, K.M. & Runcorn, S.K., Elsevier, Ámsterdam.